

STD 9.

CSEWG SHIELDING BENCHMARK SPECIFICATIONS
NEUTRON ATTENUATION MEASUREMENTS
IN A MOCKUP OF THE
FFTF RADIAL SHIELD

AEC Research and Development Report

MASTER

Anl03-M6SF00824



Atomics International
North American Rockwell

P.O. Box 309
Canoga Park, California 91304

DISCLAIMER

This report was prepared as an account of work sponsored by an agency of the United States Government. Neither the United States Government nor any agency Thereof, nor any of their employees, makes any warranty, express or implied, or assumes any legal liability or responsibility for the accuracy, completeness, or usefulness of any information, apparatus, product, or process disclosed, or represents that its use would not infringe privately owned rights. Reference herein to any specific commercial product, process, or service by trade name, trademark, manufacturer, or otherwise does not necessarily constitute or imply its endorsement, recommendation, or favoring by the United States Government or any agency thereof. The views and opinions of authors expressed herein do not necessarily state or reflect those of the United States Government or any agency thereof.

DISCLAIMER

Portions of this document may be illegible in electronic image products. Images are produced from the best available original document.

NOTICE

This report was prepared as an account of work sponsored by the United States Government. Neither the United States nor the United States Atomic Energy Commission, nor any of their employees, nor any of their contractors, subcontractors, or their employees, makes any warranty, express or implied, or assumes any legal liability or responsibility for the accuracy, completeness or usefulness of any information, apparatus, product or process disclosed, or represents that its use would not infringe privately owned rights.

STD 9

CSEWG SHIELDING BENCHMARK SPECIFICATIONS
NEUTRON ATTENUATION MEASUREMENTS
IN A MOCKUP OF THE
FFTF RADIAL SHIELD,

By
P. F. ROSE
H. ALTER
R. K. PASCHALL
A. W. THIELE



Atomics International
North American Rockwell

P.O. Box 309
Canoga Park, California 91304

CONTRACT: AT(04-3)-824
ISSUED: JANUARY 15, 1973

DISCLAIMER

This book was prepared at an account of work sponsored by an agency of the United States Government. Neither the United States Government nor any agency thereof, nor any of their employees, makes any warranty, express or implied, or assumes any legal liability or responsibility for the accuracy, completeness, or usefulness of any information, apparatus, product, or process disclosed, or represents that its use would not infringe privately owned rights. Reference herein to any specific commercial product, process, or service by trade name, trademark, manufacturer, or otherwise, does not necessarily constitute or imply its endorsement, recommendation, or favoring by the United States Government or any agency thereof. The views and opinions of authors expressed herein do not necessarily state or reflect those of the United States Government or any agency thereof.

THIS PAGE
WAS INTENTIONALLY
LEFT BLANK

CONTENTS

	Page
Abstract	4
I. Source Experiment	5
II. System Description	5
III. Calculational Model Description	7
IV. Fission Source Description	13
V. Experimental Results	15
VI. Self-Shielding Correction Factors for Foil Data	22
VII. Reporting Procedures	22
References	23
Addendum - Background Information for Shielding Benchmark of FFTF Radial Shield Mockup	25

TABLES

1. Cross Section Group Structure	6
2. Axial Mesh Description	9
3. Radial Mesh Description and Fixed Source	13
4. Group Flux Integrals - FFTF Shield Spectra	14
5. FFTF Radial Shield Foil Results (Absolute saturated dps/gm-kw fission plate power)	16

FIGURES

1. Mesh Interval Diagram and Composition (r,z) Geometry	8
2. Atom Densities for FFTF Radial Shield Benchmark (atoms/barn-cm)	12
3. FFTF Radial Shield Foil Results	
a. Aluminum Foil	17
b. Sulfur Foil	18
c. Cobalt Foil	19
d. Gold Foil	20
e. Indium Foil	21

ABSTRACT

The experimental details and the calculational specifications for a CSEWG integral data testing shielding experiment are presented. The shielding experiment described in the benchmark model is a combination of sodium and stainless steel that simulates the FFTF radial shield. The measurements in general include use of foil activation techniques using resonance and threshold detectors and proton recoil neutron spectrometer measurements in the range 5 kev to 2 Mev. The benchmark model is a test of the neutron cross-section data for sodium and the material components of stainless steel.

I. SOURCE EXPERIMENT

The neutron flux was measured in a combination of sodium and stainless steel which simulated the FFTF radial shield. Foil activation techniques, using resonance and threshold detectors, and a proton recoil neutron spectrometer (PRD), in the energy range 5 kev to 2 Mev, were used to obtain measured quantities.

II. SYSTEM DESCRIPTION

See Addendum.

TABLE 1
CROSS SECTION GROUP STRUCTURE

Group	Group Energy ΔE	Lethargy Interval Δu	Group χ Values $\chi_{^{235}g}$
1	10 Mev - 6.065 Mev	0.5	0.023716
2	6.065 Mev - 3.679 Mev		0.10436
3	3.679 Mev - 2.231 Mev		0.20050
4	2.231 Mev - 1.353 Mev		0.22630
5	1.353 Mev - 820.9 kev		0.18270
6	820.9 kev - 497.9 kev		0.11980
7	497.9 kev - 302.0 kev		0.069115
8	302.0 kev - 183.2 kev		0.036872
9	183.2 kev - 111.1 kev		0.018754
10	111.1 kev - 67.38 kev		0.92653-02
11	67.38 kev - 40.87 kev		0.44975-02
12	40.87 kev - 24.79 kev		0.21599-02
13	24.79 kev - 15.03 kev		0.10306-02
14	15.03 kev - 9.119 kev		0.48977-03
15	9.119 kev - 5.531 kev		0.23221-03
16	5.531 kev - 2.035 kev	1.0	0.11513-03
17	2.035 kev - 167.0 ev	2.5	0.455095-04
18	167 ev - 101.3 ev	0.5	0.5788-06
19	101.3 ev - 8.32 ev	2.5	0.0
20	8.32 ev - 3.06 ev	1.0	
21	3.06 ev - 1.86 ev	0.5	
22	1.86 ev - 1.13 ev	0.5	
23	1.13 ev - 0.414 ev	1.0	
24	0.414 ev - 10^{-5} ev		0.0

III. CALCULATIONAL MODEL DESCRIPTION

The benchmark model is to be calculated by two-dimensional transport theory in (r,z) geometry, with S_8 quadrature, and using 24-group cross sections to order P-3. A one-iteration fixed-source calculation will be used to obtain the flux. The flux convergence is set equal to 0.005. The multigroup scheme, lethargy interval, and group χ values are presented in Table 1. Since the benchmark model consists of large volumes of sodium and stainless steel, it is suggested that appropriate weighting spectra be used for generating the required group constants. For the stainless steel volumes, the use of iron cross-section data for generating a weighting spectra is suggested. In any event, when reporting results comparing calculation with experiment, it is requested that the method or methods used to produce the multigroup constants be detailed. The two-dimensional mesh description is shown in Figure 1. Material compositions are designated for the various regions in the figure. Beyond Mesh Interval 24, the composition is one dimensional in the axial dimension, and may be obtained from the axial mesh description in Table 2.

Atom densities for the various compositions are specified in Figure 2.

AI-AEC-13048

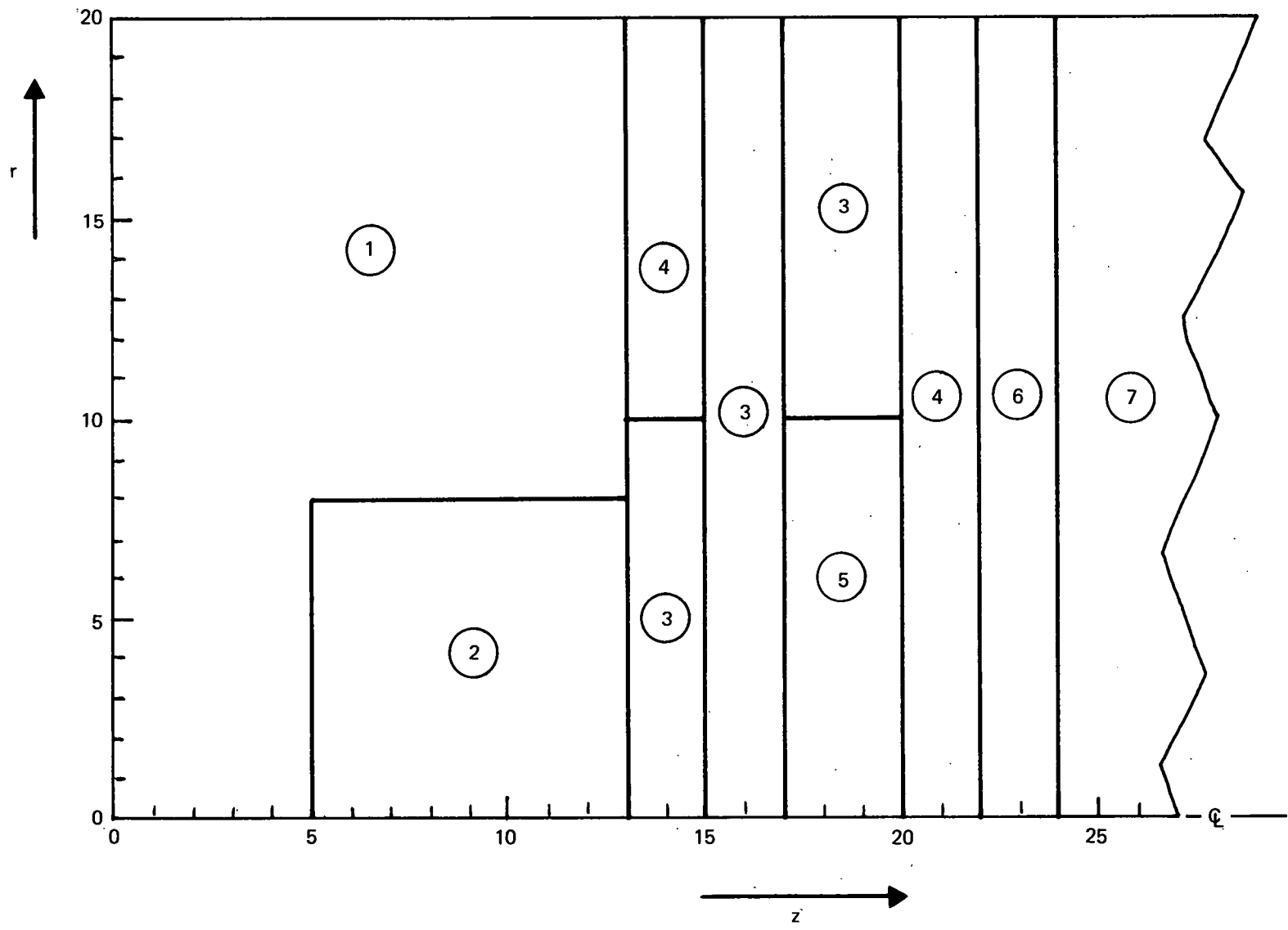


Figure 1. Mesh Interval Diagram and Composition (r, z) Geometry

6524-4671

TABLE 2
AXIAL MESH DESCRIPTION
(See Figure 4 of Addendum)
(Sheet 1 of 3)

Mesh Interval	Z (cm)	G _L Composition	Notes
1	6.0	1	Thermal column
2	12.0		
3	18.0		
4	24.0		
5	30.48		
6	36.0	2	Void cube
7	41.0		
8	46.0		
9	51.0		
10	56.0		
11	61.0		
12	66.0		
13	71.12		
14	71.28	3	Aluminum
15	71.438	3	
16	72.87	3	Aluminum - fission plate
17	74.2950	3	
18	74.3458	5	Fission plate
19	74.3966	5	
20	74.447	5	
21	74.606	4	Boral - fission plate
22	74.765	4	
23	76.000	6	Aluminum + gaps
24	77.622	6	
25	79.080	7	Stainless steel + gaps
26	80.580		
27	82.272		
28	83.772		Foil No. 2
29	85.080		
30	86.580		
31	87.932		
32	89.532		Foil No. 3
33	91.080		
34	92.580		
35	93.782		
36	95.122		Foil No. 4
37	96.680		
38	98.480		
39	99.982		
40	100.982		
41	101.980	7	PRD No. 1

TABLE 2
 AXIAL MESH DESCRIPTION
 (See Figure 4 of Addendum)
 (Sheet 2 of 3)

Mesh Interval	Z (cm)	G Composition	Notes
42	103.022	7	
43	104.292	8	
44	108.080		
45	112.580		
46	117.580		
47	122.072		
48	124.112	7	Stainless steel + gaps, PRD No. 2
49	125.112		
50	126.580		
51	128.080		
52	129.580		
53	131.080		
54	132.580		
55	134.080		
56	135.542		
57	136.542		PRD No. 3
58	137.980		
59	139.380		
60	140.780		
61	142.080		
62	143.480		
63	144.980		
64	146.380		
65	147.472		
66	152.580	9	Second sodium slab assembly
67	157.580		
68	162.617		
69	166.617		
70	171.980		PRD No. 4
71	177.380		
72	182.780		
73	188.180		
74	193.580		
75	198.980		
76	204.380		
77	209.780		
78	214.782	9	

TABLE 2
AXIAL MESH DESCRIPTION
(See Figure 4 of Addendum)
(Sheet 3 of 3)

Mesh Interval	Z (cm)	G Composition	Notes
79	216.472	11	Iron Slab, PRD No. 5
80	218.172	11	
81	219.862	11	
82	225.080	10	Third sodium slab assembly
83	230.080		
84	235.080		
85	240.080		
86	245.080		
87	250.522		
88	256.522		Foil No. 16
89	260.080		
90	265.080		
91	270.080		
92	275.080		
93	280.080		
94	284.542		
95	288.542		Foil No. 17
96	294.080		
97	299.080		
98	304.080		
99	311.080		
100	318.92	10	

ELEMENT	COMPOSITION										
	1	2	3	4	5	6	7	8	9	10	11
B				0.0395							
C	0.0802			0.00987			0.0000497				0.00019
Na								0.019805	0.022421	0.022852	
O		0.00001									
N		0.00004									
Al		0.0602	0.0384		0.00668		0.004036	0.002271	0.002319		
Fe						0.05299					0.08459
Ni						0.00787					
Cr						0.01408					
Cu						0.000099					
Mo						0.000133					
Si						0.000193					
Mn						0.00103					
U ²³⁵				0.0448							
U ²³⁸				0.00325							

6524-4672

Figure 2. Atom Densities for FFTF Radial Shield Benchmark (atoms/barn-cm)

IV. FISSION SOURCE DESCRIPTION

In order to specify a fixed source, S_i , for a volume element of the fission plate, a radial fission activity plot was made on the back of the fission plate, using fully enriched U^{235} foils. The relative activity, $a_{i-1/2}$, was obtained at the center of each radial mesh interval. These activities were then normalized, so that the source integral is 1 neutron/sec. For this benchmark calculation, it is assumed that the source is flat, axially. Then:

$$S_i = \frac{a_{i-1/2}}{d \sum a_{i-1/2} (r_i^2 - r_{i-1}^2)} , \quad \dots (1)$$

where d , the fission plate thickness, equals 0.1524 cm. S_i is tabulated in Table 3. S_i by interval, is to be multiplied by χ_j to obtain the fixed source in Energy Group j .

TABLE 3
RADIAL MESH DESCRIPTION AND FIXED SOURCE

Mesh Interval	r (cm)	Fission Plate Source* (1 neutron/sec)
1	2.86625	0.010313
2	5.7325	0.010275
3	8.59875	0.0101765
4	11.4650	0.01006496
5	14.33125	0.0097802
6	17.19750	0.0093097
7	20.06375	0.0085052
8	22.93000	0.00742848
9	26.70500	0.00534829
10	30.48	0.0038750
11	36.032	
12	41.584	
13	47.136	
14	52.688	
15	58.240	
16	63.792	
17	69.344	
18	74.896	
19	80.448	
20	86.000	

*For all detector data, 7.49×10^{13} neutrons/sec normalizes the calculation to 1-kw fission plate (F. P.) power, as used in the data reported in the benchmark specification.

TABLE 4
GROUP FLUX INTEGRALS - FFTF SHIELD SPECTRA

Group	Detector			
	0.8 atm H ₂	2.63 atm H ₂ + 0.263 atm CH ₄	2.63 atm CH ₄	8.1 atm CH ₄
<u>Detector Position = 25.4 cm</u>				
	(x 10 ⁸)	(x 10 ⁹)	(x 10 ⁹)	(x 10 ⁹)
3				
4				0.849 ± 0.048
5				1.648 ± 0.041
6			2.686 ± 0.062	
7			3.039 ± 0.046	
8		2.784 ± 0.077		
9		2.582 ± 0.048		
10	20.450 ± 0.744	1.975 ± 0.030		
11	15.069 ± 0.461	1.664 ± 0.016		
12	13.021 ± 0.311			
13	12.785 ± 0.174			
14	9.197 ± 0.081			
15	6.397 ± 0.038			
<u>Detector Position = 49.54 cm</u>				
	(x 10 ⁸)	(x 10 ⁸)	(x 10 ⁸)	(x 10 ⁸)
4				1.238 ± 0.096
5				2.536 ± 0.083
6			4.959 ± 0.139	
7			8.964 ± 0.128	
8		10.356 ± 0.251		
9		10.684 ± 0.169		
10	10.309 ± 0.271	9.637 ± 0.114		
11	8.354 ± 0.190	8.898 ± 0.066		
12	6.966 ± 0.142			
13	7.272 ± 0.087			
14	5.522 ± 0.043			
15	4.077 ± 0.021			
<u>Detector Position = 60.94 cm</u>				
	(x 10 ⁸)	(x 10 ⁸)	(x 10 ⁸)	(x 10 ⁸)
4				0.282 ± 0.029
5				0.770 ± 0.028
6			1.765 ± 0.050	
7			3.363 ± 0.045	
8		4.521 ± 0.102		
9		5.049 ± 0.070		
10	4.490 ± 0.124	4.417 ± 0.048		
11	4.049 ± 0.113	4.326 ± 0.028		
12	3.551 ± 0.098			
13	3.638 ± 0.060			
14	2.677 ± 0.029			
15	1.977 ± 0.014			
<u>Detector Position = 89.54 cm</u>				
	(x 10 ⁷)	(x 10 ⁷)	(x 10 ⁷)	(x 10 ⁷)
4				0.212 ± 0.034
5				0.639 ± 0.034
6				1.813 ± 0.034
7			1.576 ± 0.065	
8		8.129 ± 0.186		
9		11.392 ± 0.149		
10	11.628 ± 0.256	12.277 ± 0.112		
11	9.674 ± 0.218	11.690 ± 0.070		
12	9.758 ± 0.179			
13	10.190 ± 0.114			
14	8.222 ± 0.057			
15	4.849 ± 0.028			
<u>Detector Position = 142.24 cm</u>				
	(x 10 ⁷)	(x 10 ⁷)		
8		0.500 ± 0.015		
9		0.906 ± 0.024		
10	1.458 ± 0.033	1.466 ± 0.012		
11	1.455 ± 0.033	2.011 ± 0.009		
12	2.012 ± 0.029			
13	1.992 ± 0.020			
14	1.681 ± 0.011			
15	1.198 ± 0.005			

V. EXPERIMENTAL RESULTS

The measured values of the FFTF shield spectra were integrated as appropriate, and group flux integrals, defined by

$$\phi_g = \int_{\Delta u_g} \phi(u) du , \quad \dots (2)$$

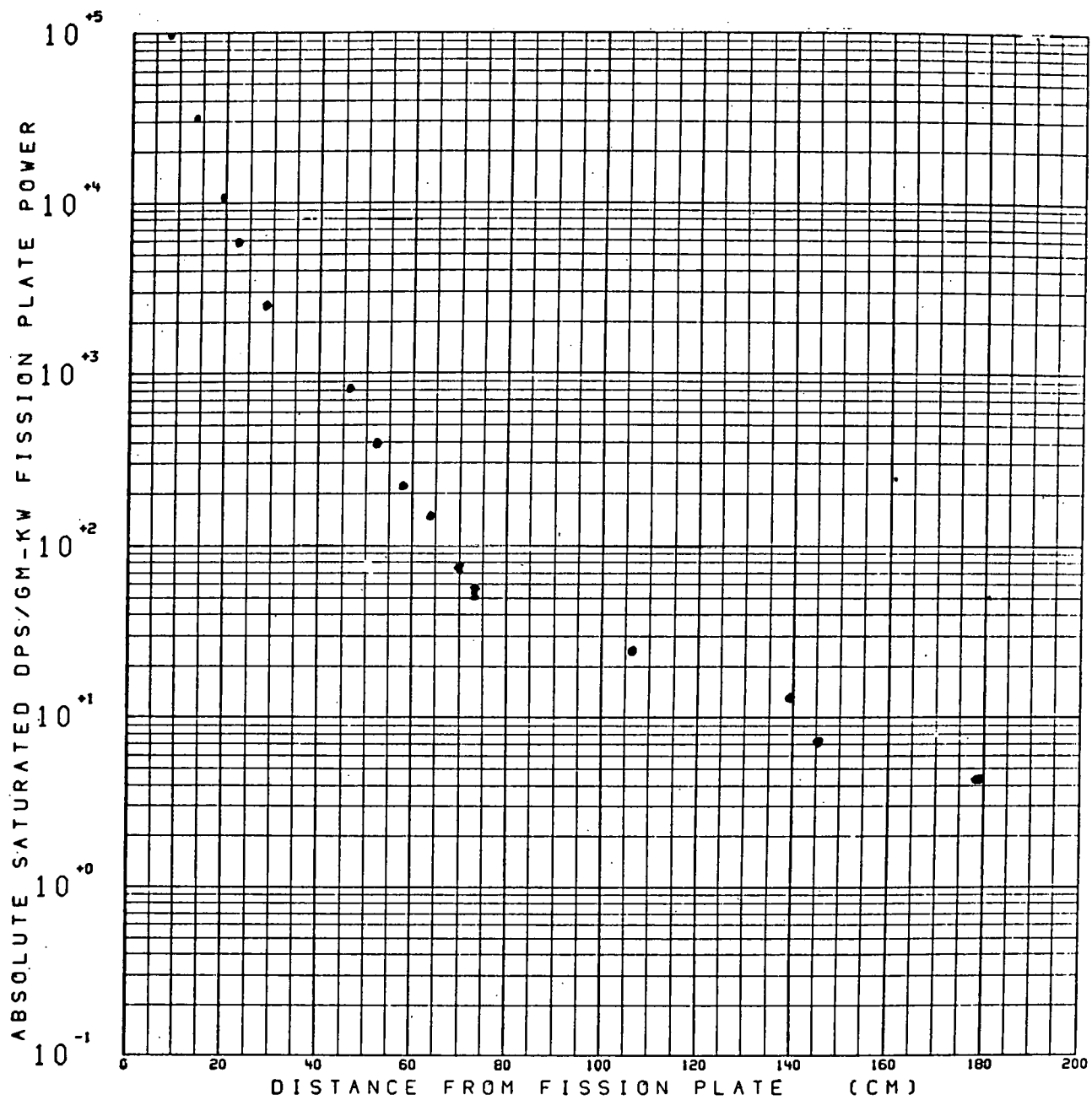
were obtained at the several detector positions. These group values, presented in Table 4, were obtained from Tables 3 through 6 in the Addendum.

Table 5 shows a tabulation of FFTF radial shield foil activities as a function of axial position, with corresponding plots shown in Figures 3a through 3e.

TABLE 5

FFTF RADIAL SHIELD FOIL RESULTS
(Absolute saturated dps/gm-kw fission plate power)

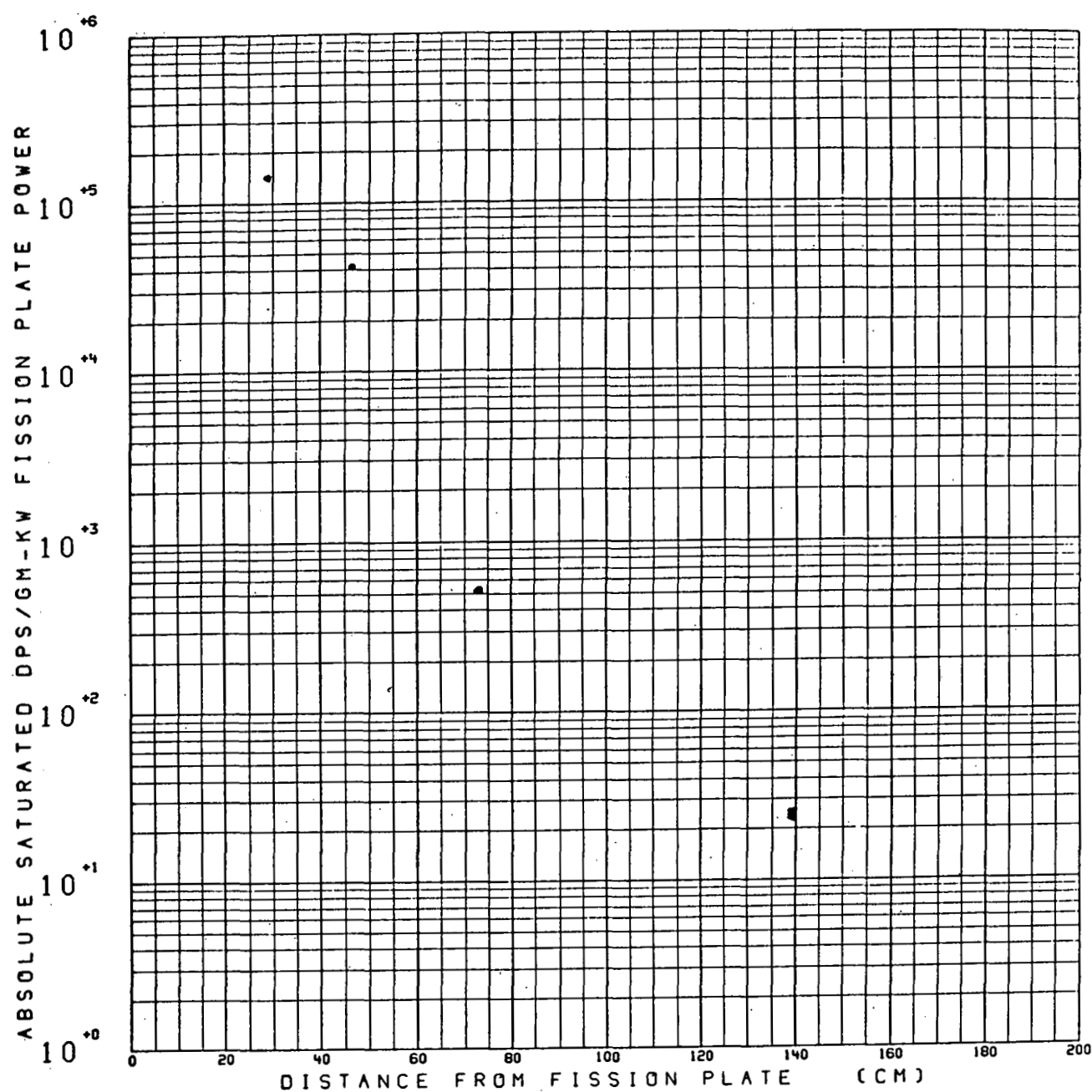
Z (cm)	Al	S	Co	Au	In
1.27	$\sim 5.0 + 5$	$\sim 3.3 + 7$		$2.403 + 9$ $\pm 2.99 + 6$	$3.42 + 9$ $\pm 3.76 + 6$
7.94	$9.632 + 4$ $\pm 1.32 + 2$		$5.816 + 8$ $\pm 2.21 + 6$	$2.473 + 9$ $\pm 3.10 + 6$	$2.64 + 9$ $\pm 2.45 + 6$
13.65	$3.123 + 4$ $\pm 7.50 + 1$		$5.413 + 8$ $\pm 2.13 + 6$	$2.144 + 9$ $\pm 2.83 + 6$	$2.16 + 9$ $\pm 2.12 + 6$
19.37	$1.064 + 4$ $\pm 4.45 + 1$		$4.483 + 8$ $\pm 1.94 + 6$	$1.841 + 9$ $\pm 2.72 + 6$	$1.99 + 9$ $\pm 1.30 + 6$
22.54	$5.826 + 3$ $\pm 3.27 + 1$		$3.720 + 8$ $\pm 1.77 + 6$	$1.575 + 9$ $\pm 3.52 + 6$	$1.68 + 9$ $\pm 3.19 + 6$
28.58	$2.482 + 3$ $\pm 2.15 + 1$	$1.429 + 5$ $\pm 2.51 + 2$	$2.988 + 8$ $\pm 1.58 + 6$	$1.251 + 9$ $\pm 3.15 + 6$	$1.39 + 9$ $\pm 2.32 + 6$
46.36	$8.048 + 2$ $\pm 1.22 + 1$	$4.109 + 4$ $\pm 1.36 + 2$	$2.749 + 8$ $\pm 1.52 + 6$	$1.137 + 9$ $\pm 2.99 + 6$	$1.164 + 9$ $\pm 9.48 + 5$
52.39	$3.931 + 2$ $\pm 8.43 + 0$		$2.101 + 8$ $\pm 1.32 + 6$	$8.618 + 8$ $\pm 2.59 + 6$	$8.755 + 8$ $\pm 8.11 + 5$
58.10	$2.225 + 2$ $\pm 6.28 + 0$		$1.457 + 8$ $\pm 1.10 + 6$	$5.979 + 8$ $\pm 1.52 + 6$	$6.379 + 8$ $\pm 6.88 + 5$
63.82	$1.481 + 2$ $\pm 5.04 + 0$		$1.045 + 8$ $\pm 8.96 + 5$	$4.702 + 8$ $\pm 1.34 + 6$	$5.076 + 8$ $\pm 6.04 + 5$
69.53	$7.484 + 1$ $\pm 3.36 + 0$		$6.942 + 7$ $\pm 7.29 + 5$	$3.001 + 8$ $\pm 1.07 + 6$	$3.182 + 8$ $\pm 4.70 + 5$
73.03	$5.398 + 1$ $\pm 2.74 + 0$	$5.161 + 2$ $\pm 1.36 + 1$	$5.485 + 7$ $\pm 6.45 + 5$	$2.382 + 8$ $\pm 9.69 + 5$	$2.643 + 8$ $\pm 2.74 + 5$
106.05	$2.494 + 1$ $\pm 5.16 - 1$		$4.108 + 7$ $\pm 5.57 + 5$	$1.608 + 8$ $\pm 7.92 + 5$	$2.029 + 8$ $\pm 2.37 + 5$
139.07	$1.310 + 1$ $\pm 3.23 - 1$	$2.432 + 1$ $\pm 1.32 + 0$	$2.783 + 7$ $\pm 4.59 + 5$	$1.114 + 8$ $\pm 6.65 + 5$	$1.425 + 8$ $\pm 1.93 + 5$
145.42	$7.199 + 0$ $\pm 2.03 - 1$		$1.370 + 7$ $\pm 3.16 + 5$	$5.451 + 7$ $\pm 4.56 + 5$	$7.202 + 7$ $\pm 1.38 + 5$
178.44	$4.375 + 0$ $\pm 1.32 - 1$		$7.029 + 6$ $\pm 2.21 + 5$	$3.122 + 7$ $\pm 3.44 + 5$	$4.666 + 7$ $\pm 1.10 + 5$
211.48			$2.729 + 6$ $\pm 1.28 + 5$	$1.471 + 7$ $\pm 2.40 + 5$	$2.356 + 7$ $\pm 7.57 + 4$



6524-4673

a. Aluminum Foil

Figure 3. FFTF Radial Shield Foil Results
(Sheet 1 of 5)

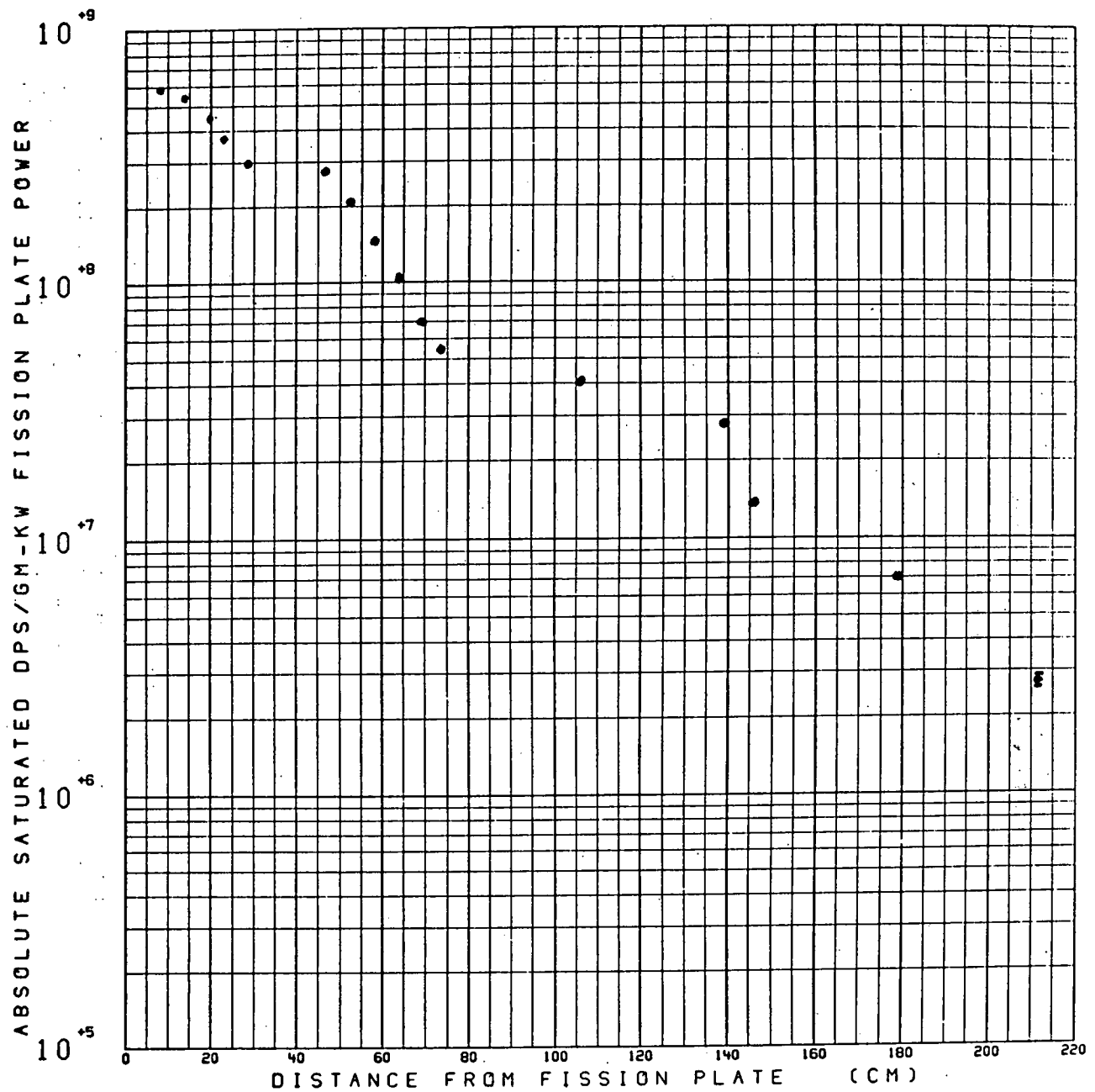


6524-4674

b. Sulfur Foil

Figure 3. FFTF Radial Shield Foil Results
(Sheet 2 of 5)

AI-AEC-13048

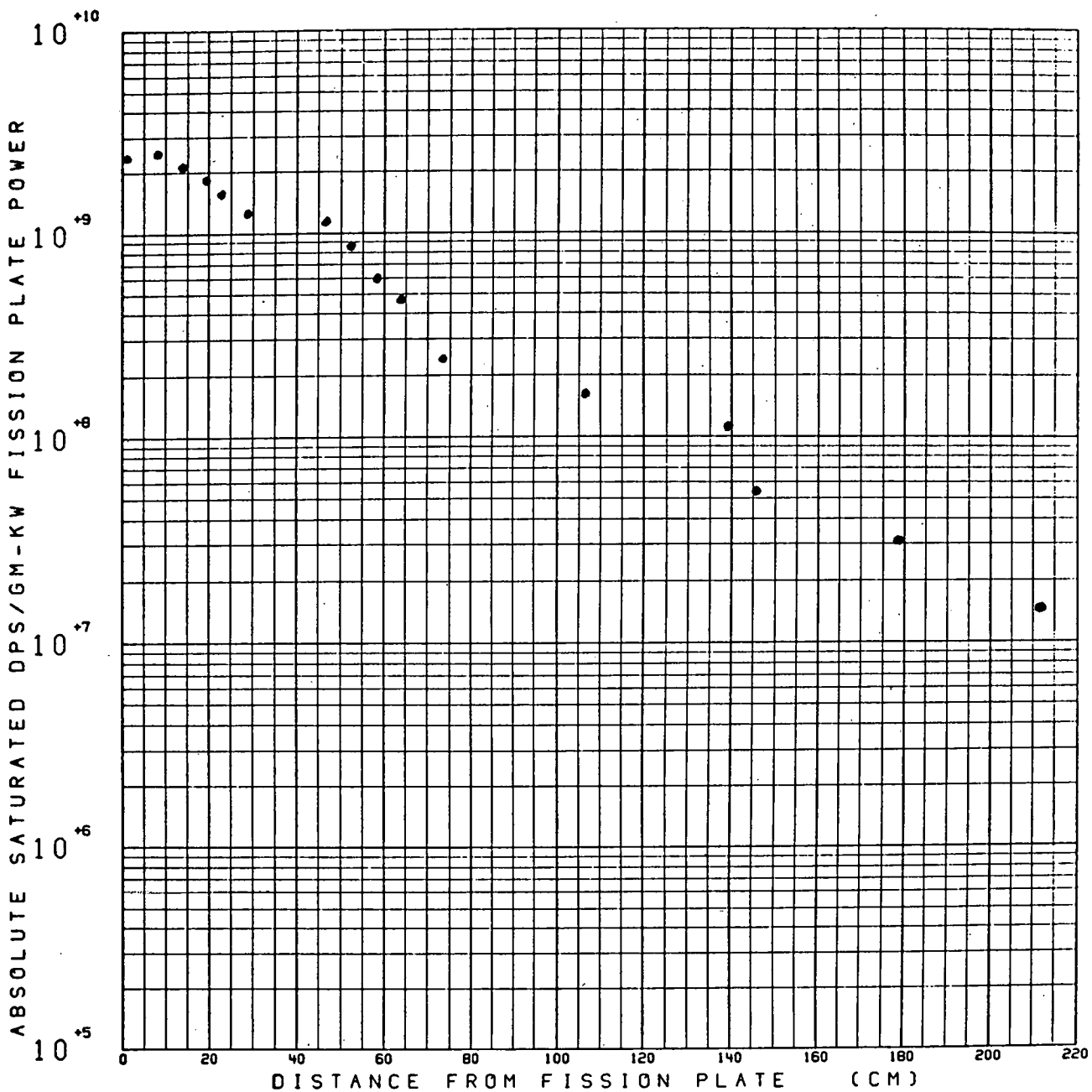


6524-4675

c. Cobalt Foil

Figure 3. FFTF Radial Shield Foil Results
(Sheet 3 of 5)

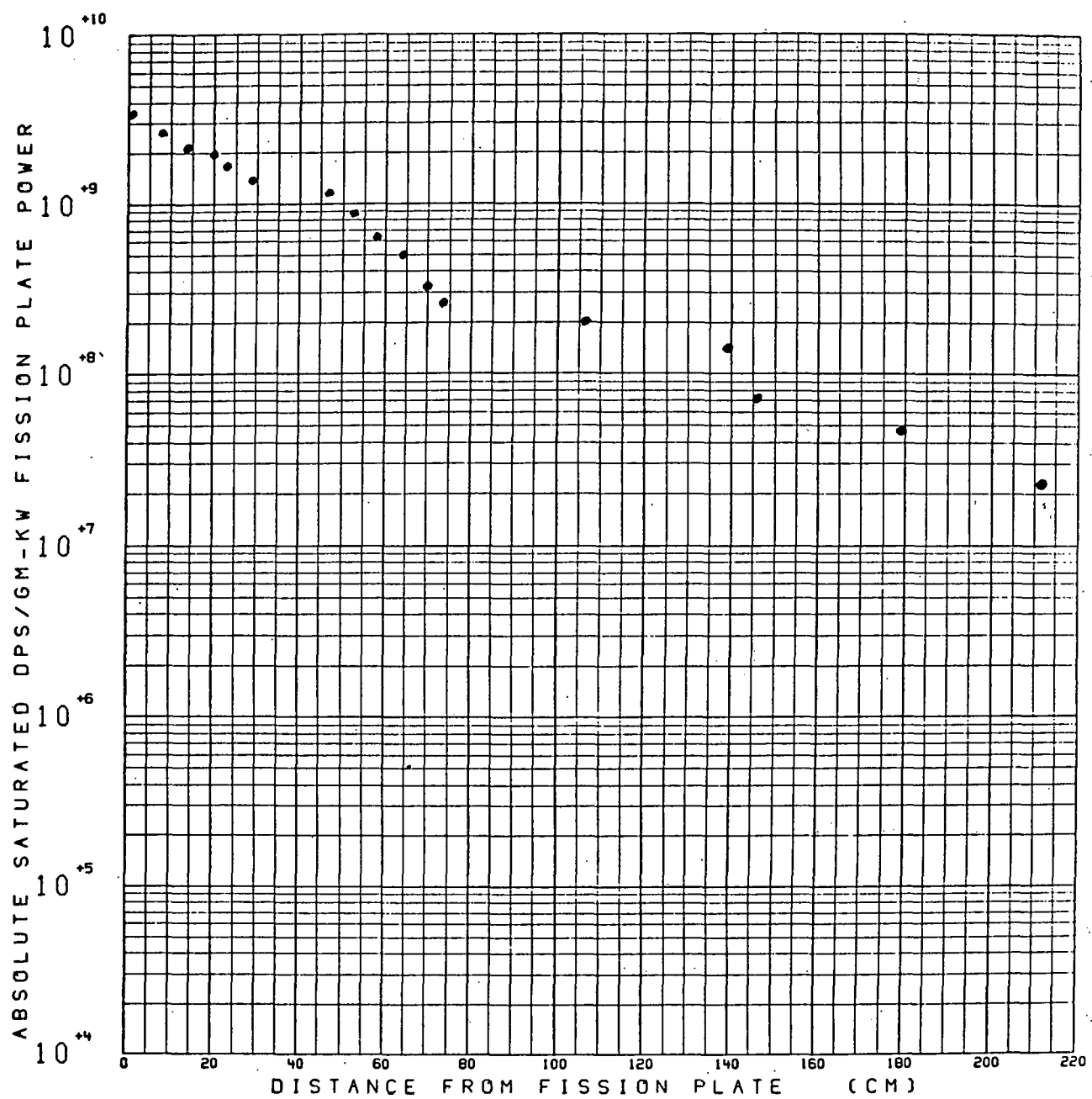
AI-AEC-13048



6524-4676

d. Gold Foil

Figure 3. FFTF Radial Shield Foil Results
(Sheet 4 of 5)



6524-4677

e. Indium Foil

Figure 3. FFTF Radial Shield Foil Results
(Sheet 5 of 5)

VI. SELF-SHIELDING CORRECTION FACTORS FOR FOIL DATA

The activities of indium, cobalt, and gold were corrected for self-shielding, using the data in References 1 and 2. Indium and cobalt corrections were obtained from Reference 1, while the data from Reference 2 were used for gold. The correction factors used were as follows:

	<u>Thermal</u>	<u>Epithermal</u>
Indium	1.147	5.23
Cobalt	1.089	2.46
Gold	1.216	5.46

The dead-time corrected activity was multiplied by the correction factor to get the non-self-shielded activity.

VII. REPORTING PROCEDURES

Calculated group flux integrals should be compared with the similar experimental values given in Table 4. A listing of the comparisons, side by side, will be sufficient.

In a similar fashion, the calculated foil results should be given in a comparison listing.

All results reported by the data-testing participants will be assembled, and a report issued.

It is imperative that each participant report in some detail any deviation from benchmark model specifications, in order that discrepancies in reported results, if any, may be explained.

REFERENCES

1. K. G. Randen, "Conventions and Procedures for Neutron Flux Measurements Using Foil Techniques at the STIR Facility," NAA-SR-TDR-10628 (October 29, 1964)
2. L. S. Beller and H. Farrar IV, "Effective Integrals and Attenuation Factors for Gold," NAA-SR-MEMO-12164 (September 20, 1966)

THIS PAGE
WAS INTENTIONALLY
LEFT BLANK

ADDENDUM
BACKGROUND INFORMATION FOR SHIELDING BENCHMARK OF FFTF
RADIAL SHIELD MOCKUP

THIS PAGE
WAS INTENTIONALLY
LEFT BLANK

CONTENTS

	Page
I. Introduction	29
II. Test Configuration	29
A. Radiation Source	29
B. Test Shields	31
C. FFTF Radial Shield	33
III. Measurement Techniques	38
A. Foil Measurements	38
B. Proton Recoil Neutron Spectra Measurements	38
IV. Results	41
References	52

TABLES

1. Geometry and Composition of Experimental Configuration	35
2. Detector Fillings and Energy Limits	40
3. FFTF Shield Spectra - $\phi(u)$ at 1-kw F. P. Power (0.8 atm H ₂ Detector)	43
4. FFTF Shield Spectra - $\phi(u)$ at 1-kw F. P. Power (2.63 atm H ₂ + 0.263 atm CH ₄ Detector)	44
5. FFTF Shield Spectra - $\phi(u)$ at 1-kw F. P. Power (2.63 atm CH ₄ Detector)	45
6. FFTF Shield Spectra - $\phi(u)$ at 1-kw F. P. Power (8.1 atm CH ₄ Detector)	46

FIGURES

	Page
1. Shield Test Arrangement	30
2. Details of Fission Plate	30
3. Typical Test Shield Configuration	32
4. FFTF Radial Shield Mockup Configuration	34
5. Neutron Spectra in FFTF Radial Shield	42
6. Effect of LiH Interrupt on Neutron Spectrum in FFTF Radial Shield	47
7. Activation in FFTF Radial Shield	
a. Indium Foil	48
b. Gold Foil	48
c. Cobalt Foil	48
8. Activation in FFTF Radial Shield	
a. Sulfur Foil	49
b. Aluminum Foil	49
9. Vertical Traverses in FFTF Radial Shield	
a. Gold Foils, Position 2, 13.7 cm From Fission Plate	50
b. Gold Foils, Position 8, 58.1 cm From Fission Plate	50
c. Gold Foils, Position 13, 139.1 cm From Fission Plate	50
d. Gold Foils, Position 15, 178.1 cm From Fission Plate	51
e. Sulfur Foils, Position 5, 28.6 cm From Fission Plate	51
f. Sulfur Foils, Position 11, 73.0 cm From Fission Plate	51

I. INTRODUCTION

A series of neutron attenuation measurements has been made in test shields of sodium, and of sodium-and-steel. These measurements are a part of a continuing program of study on fast reactor shield performance.⁽¹⁻³⁾ It is the objective of this program to provide experimental data on the radiation attenuation properties that will assist the designer in evaluating both the accuracy of the nuclear data and of his analytical methods. It is not intended that the shield studies are to be exact prototypes of planned reactor shield systems; but rather that they be representative combinations of materials, so arranged that they lend themselves to a good simulation of an analytical model. A comparison of the experimental and analytical results will serve to establish a limit on the uncertainty in shield performance.

The shielding experiment described in the benchmark is a combination of sodium and stainless steel that simulates the FFTF radial shield.⁽³⁾ The measurements, in general, include the use of foil activation techniques, using resonance and threshold detectors, and proton recoil neutron spectrometer measurements in the range 5 kev to 2 Mev. The experimental data are the significant end product of this program.

II. TEST CONFIGURATION

A. RADIATION SOURCE

The radiation source for all the measurements described here was the fission plate of the Shield Test and Irradiation Reactor. The reactor is a 1-Mw pool-type reactor, fueled with a 4 x 5 array of MTR plate-type fuel elements. Immediately adjacent to one side of the reactor is a graphite thermal column, 5 ft square by 4 ft long. The fission plate, a 24-in. diameter by 0.060-in. thick disc of enriched uranium-235, is centered on the face of the thermal column. This arrangement is shown in Figure 1. A more complete description of the facility is contained in Reference 4.

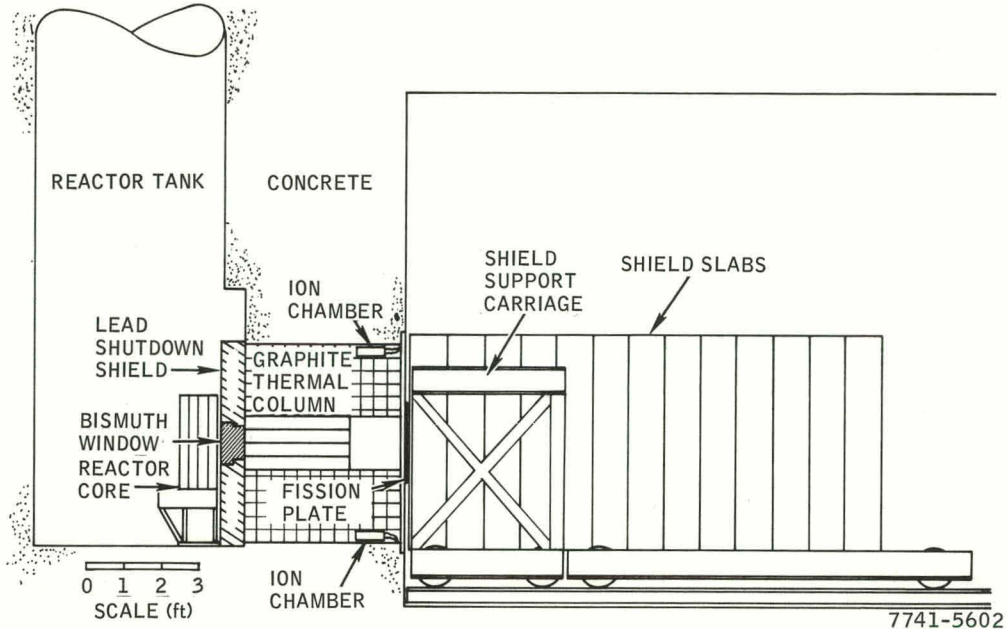


Figure 1. Shield Test Arrangement

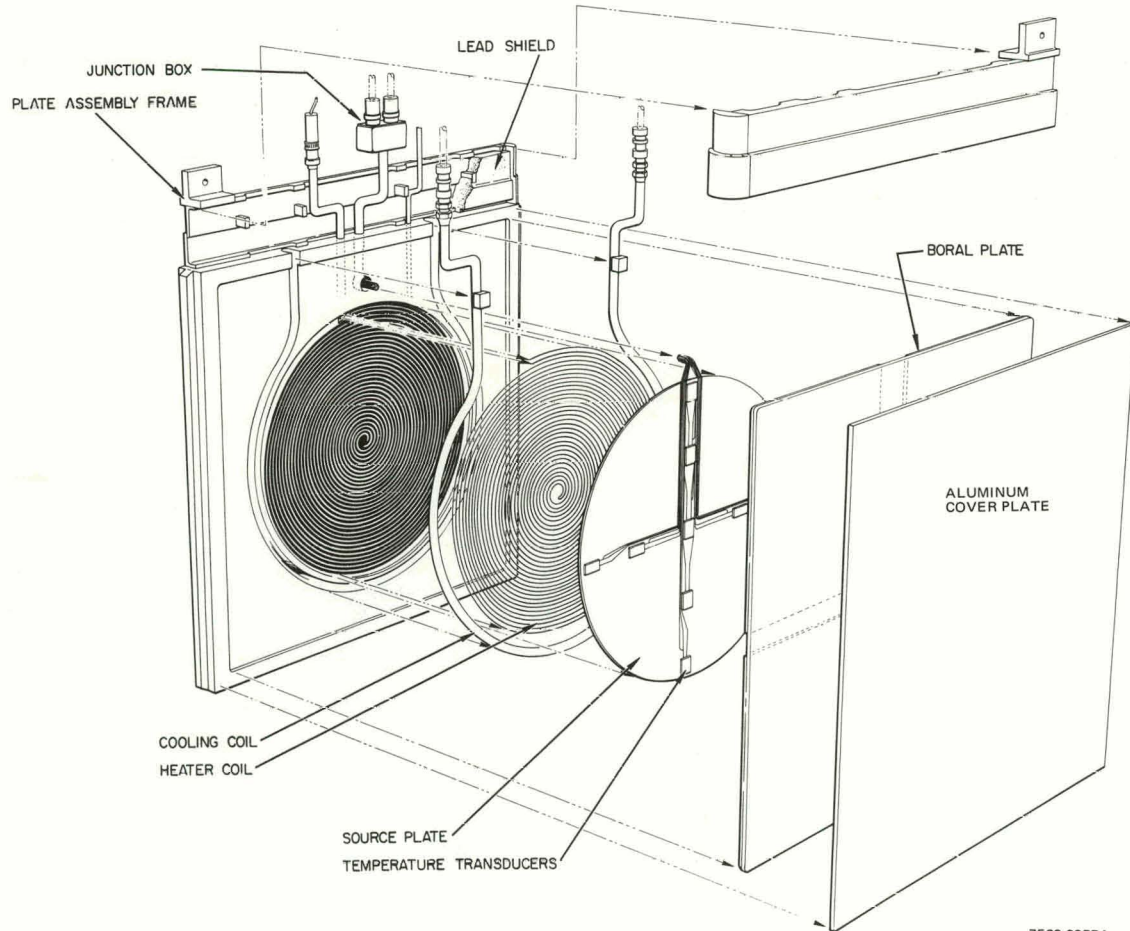


Figure 2. Details of Fission Plate

The details of the fission plate are shown in Figure 2. There is a 1-1/8-in. thick aluminum plate on the thermal column side of the fission plate, in which is mounted an electrical heater for thermal calibration and a cooling coil for heat removal. The fission plate is covered with a 1/8-in. thick boral plate and a 1/8-in. thick aluminum plate. The overall assembly is 33-3/4 in. wide by 33 in. high. The face of the thermal column is covered by a 1/8-in. thick boral plate, in which there is a 27-in. square opening (filled with aluminum).

B. TEST SHIELDS

The test shields consist of slabs of the test materials, arranged on a carriage and positioned adjacent to the fission plate, as shown in Figure 3. The materials used include the following:

- 1) Sodium - The sodium slabs consist of a 60 by 60 by 12 in. slab of sodium, clad in 6061T6 aluminum. The aluminum is 1/4 in. thick in the 12 in. dimension, so that the total thickness of each slab is 12-1/2 in. One slab with 6 in. of sodium was made as a part of this set. The sodium used was reactor-grade material. Details of the fabrication of these slabs are contained in Reference 1.
- 2) Iron - The iron slabs are commercial-grade 1020 steel (0.2% carbon in iron). They are 60 by 66 in., with the longer dimension vertical. There are six 1/2-in., six 1-in., and six 2-in. thick slabs.
- 3) Stainless Steel - Plates of Type 304 stainless steel, 1 and 2 in. thick with transverse dimensions of 60 by 60 in. were used. The average composition, from the vendor's analysis report, was as follows:

<u>Element</u>	<u>wt %</u>
C	0.058
Mn	1.43
P	0.023
S	0.015
Si	0.43
Cu	0.13
Ni	9.58
Cr	18.76
Mo	0.23
Fe	Balance

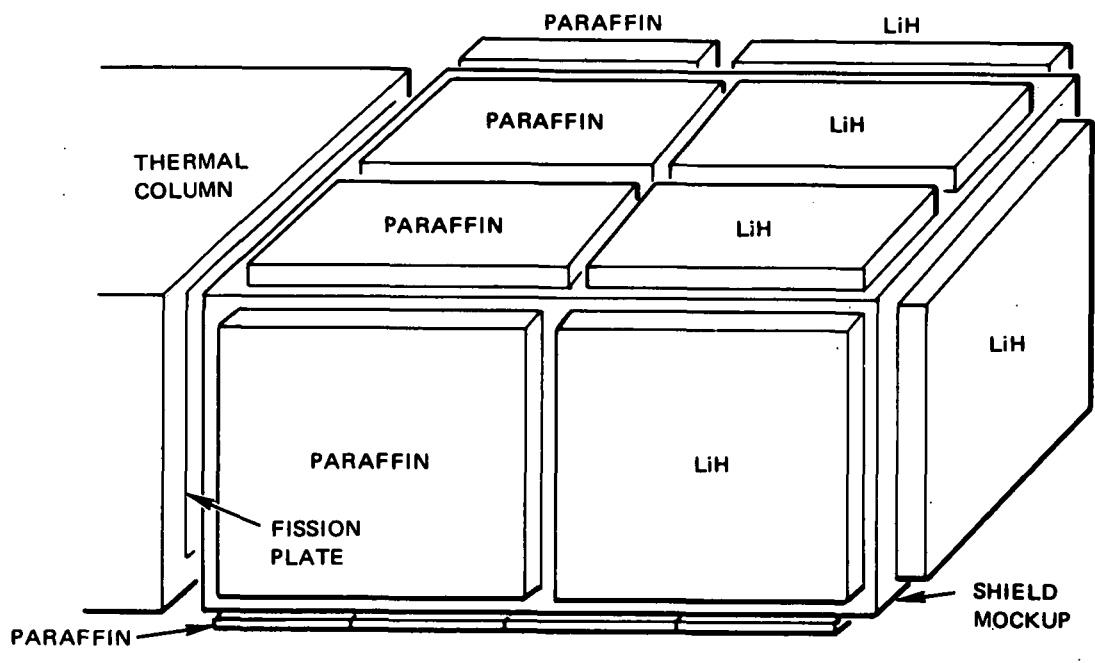


Figure 3. Typical Test Shield Configuration

Holes were cut into: (1) the 2 in. stainless steel, (2) one 2 in. iron, and (3) two sodium slabs, for insertion of the neutron spectrometer. In the steel and iron, these were 2-in. square slots, extending from the top to slightly below the center. When the detector was not in the hole, it was filled with the original material. The sodium slabs had 2-in. diameter holes, lined with thin wall aluminum tube, and filled with aluminum when not in use.

C. FFTF RADIAL SHIELD

A shield representative of the materials in the radial direction of the FFTF was studied. The materials used included the following:

9 in. stainless steel
6 in. sodium
9 in. stainless steel
24 in. sodium
2 in. iron
36 in. sodium

The 2 in. of iron corresponds to the reactor vessel position. The dimensions of this assembly are given in Figure 4, and listed in Table 1. Two 6 in. lithium hydride slabs were substituted for the first 12 in. sodium slab, when checking the room return background.

In all these tests, additional shielding was used around the assembly to attenuate neutrons escaping from the test shield in a high flux region, scattering from the walls of the room, and returning to the shield in a region of low flux to contribute a background error.

Lithium hydride slabs, 5 ft square by 7 in. thick, were placed along the sides of the front half of the assembly. Five-foot square by 2-in. thick lithium hydride plus 1/4-in. thick boral slabs were placed along the back half of the assembly. Three-inch thick paraffin slabs and borated polyethylene were placed on top, and 2 in. of paraffin and lithium hydride were placed underneath the assembly. A 6-in. thick lithium hydride slab was placed on the back of the assembly. It was found, in the tests, that these shields were effective in reducing the wall scatter background error. In some tests, paraffin was substituted for lithium hydride, and no change was found in the measured results.

NOTE: ALL SLABS 152.4 cm SQUARE

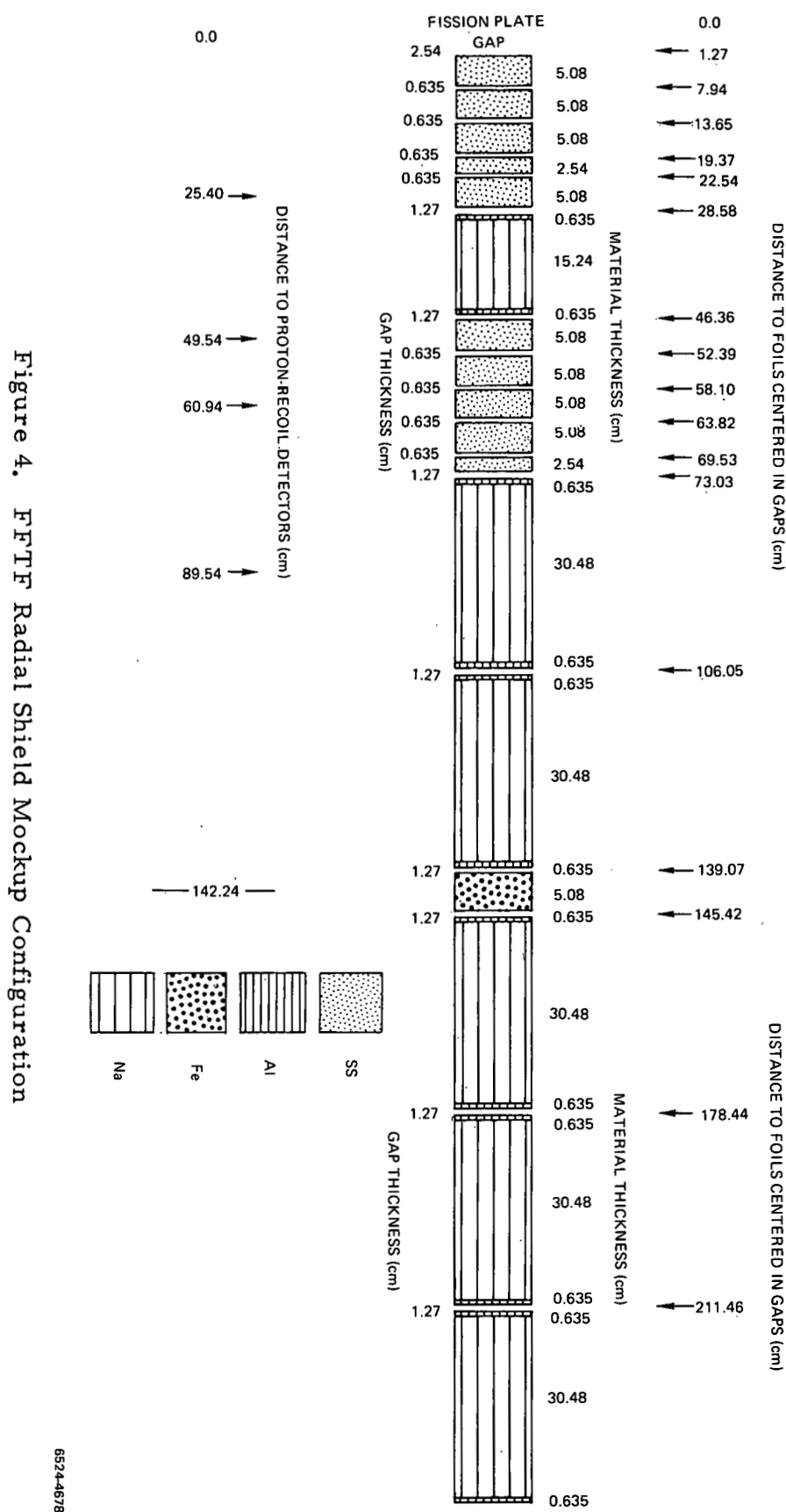


Figure 4. FFTF Radial Shield Mockup Configuration

TABLE 1
GEOMETRY AND COMPOSITION OF EXPERIMENTAL CONFIGURATION
(Sheet 1 of 3)

Zone	Thickness (cm)	Description	Composition	Atom Density (10^{24} atoms/cm 3)
1	81.28	Thermal Column	C (a)	0.0802 (b)
2	40.64	Void Cube in Thermal Column	(c)	
3	0.3175	Al Square in Boral Sheet	Al (d)	0.0602 (e)
4	2.8575	Fission Plate Assembly	Al (f)	0.0602 (e)
5	0.1524	Fission Plate Assembly	$\left\{ \begin{array}{l} \text{U}^{235} (\text{g}) \\ \text{U}^{238} (\text{g}) \end{array} \right.$	0.0448 (h)
		Fission Plate Assembly	$\left\{ \begin{array}{l} \text{B} (\text{f}) \\ \text{C} (\text{f}) \end{array} \right.$	0.00325 (h)
6	0.3175	Fission Plate Assembly	$\left\{ \begin{array}{l} \text{C} (\text{f}) \\ \text{Al} (\text{f}) \end{array} \right.$	0.0395 (i)
		Fission Plate Assembly		0.00987 (i)
7	0.3175	Fission Plate Assembly	Al (f)	0.0384 (i)
8	2.54	Gap		
9	5.08	Type 304 SS	SS (j)	(j)
10	0.635	Gap		
11	5.08	Type 304 SS	SS (j)	(j)
12	0.635	Gap		
13	5.08	Type 304 SS	SS (j)	(j)
14	0.635	Gap		
15	2.54	Type 304 SS	SS (j)	(j)
16	0.635	Gap		
17	5.08	Type 304 SS	SS (j)	(j)
18	1.27	Gap		
19	0.635	Na Slab Assembly	Al	0.0602 (k)
20	15.24	Na Slab Assembly	Na	0.0248 (l)
21	0.635	Na Slab Assembly	Al	0.0602 (k)
22	1.27	Gap		
23	5.08	Type 304 SS	SS (j)	(j)
24	0.635	Gap		
25	5.08	Type 304 SS	SS (j)	(j)

TABLE 1
GEOMETRY AND COMPOSITION OF EXPERIMENTAL CONFIGURATION
(Sheet 2 of 3)

Zone	Thickness (cm)	Description	Composition	Atom Density (10^{24} atoms/cm 3)
26	0.635	Gap		
27	5.08	Type 304 SS	SS (j)	(j)
28	0.635	Gap		
29	5.08	Type 304 SS	SS (j)	(j)
30	0.635	Gap		
31	2.54	Type 304 SS	SS (j)	(j)
32	1.27	Gap		
33	0.635	Na Slab Assembly	Al	0.0602 (k)
34	30.48	Na Slab Assembly	Na	0.0248 (l)
35	0.635	Na Slab Assembly	Al	0.0602 (k)
36	1.27	Gap		
37	0.635	Na Slab Assembly	Al	0.0602 (k)
38	30.48	Na Slab Assembly	Na	0.0248 (l)
39	0.635	Na Slab Assembly	Al	0.0602 (k)
40	1.27	Gap		
41	5.08	Fe Slab	Fe (m)	0.0848 (n)
42	1.27	Gap		
43	0.635	Na Slab Assembly	Al	0.0602 (k)
44	30.48	Na Slab Assembly	Na	0.0248 (l)
45	0.635	Na Slab Assembly	Al	0.0602 (k)
46	1.27	Gap		
47	0.635	Na Slab Assembly	Al	0.0602 (k)
48	30.48	Na Slab Assembly	Na	0.0248 (l)
49	0.635	Na Slab Assembly	Al	0.0602 (k)
50		Gap		
51	0.635	Na Slab Assembly	Al	0.0602 (k)
52	30.48	Na Slab Assembly	Na	0.0248 (l)
53	0.635	Na Slab Assembly	Al	0.0602 (k)

TABLE 1
GEOMETRY AND COMPOSITION OF EXPERIMENTAL CONFIGURATION
(Sheet 3 of 3)

NOTES:

- (a) 152.4 cm square
- (b) Assumes AGOT graphite with density $\rho = 1.7 \text{ gm/cm}^3$ is stacked with small gaps, so that effective $\rho = 1.6$
- (c) 40.64-cm square void (40.64 cm thick); outside of void is graphite, 152.4 cm square
- (d) 68.58-cm square aluminum; outside of aluminum is Boral, 152.4 cm square
- (e) Assumes pure aluminum, with theoretical density $\rho = 2.699 \text{ gm/cm}^3$
- (f) 85.725 cm wide, 83.82 cm high
- (g) 60.96 cm diameter
- (h) Fission plate uranium has 93.17% U^{235}
measured mass $U^{235} = 7800 \text{ gm}$
volume = $\pi(30.48^2) \times 0.1524 = 444.8 \text{ cm}^3$ } $\rho = \frac{7800}{444.8} = 17.5 \text{ gm/cm}^3$
- (i) Boral plate 35% B_4C , 65% Al by weight
- (j) Plates of Type 304 SS (152.4 cm square)

Average composition (wt %), from vendor's analysis report, was:

C	0.058	Cu	0.13
Mn	1.43	Ni	9.58
P	0.023	Cr	18.76
S	0.015	Mo	0.23
Si	0.43	Fe	Balance

- (k) Aluminum cladding, 152.4 cm square
Assumes pure aluminum, with theoretical density $\rho = 2.699 \text{ gm/cm}^3$
Actual material was 6061 T-6 Al
- (l) Sodium slab, 152.4 cm square
measured sodium density $\rho = 0.945 \text{ gm/cm}^3$
- (m) Iron slab, 1020 steel (0.2% carbon in iron)
167.64 cm high, 152.4 cm wide
- (n) Assumes iron theoretical density $\rho = 7.86$

III. MEASUREMENT TECHNIQUES

A. FOIL MEASUREMENTS

Foil activation techniques were used to measure the distribution of neutrons in the resonance region of 1 to 300 ev and the threshold region of 1 to 10 Mev. The reactions used include the following:

In ¹¹⁵	(n,γ)	In ¹¹⁶	1.46 ev
Au ¹⁹⁷	(n,γ)	Au ¹⁹⁸	4.91 ev
Co ⁵⁹	(n,γ)	Co ⁶⁰	132 ev
S ³²	(n,p)	p ³²	>3 Mev
Al ²⁷	(n,α)	Na ²⁴	>8.1 Mev

The foils were beta counted on scintillation counters, and the counting rates were converted to saturated activities by using a computer data reduction code. All activities were adjusted to a standard irradiation condition of 1-kw fission plate power. This adjustment was made by using the signals from the four neutron ionization chambers in the thermal column as secondary standards for flux calibration.

The detection efficiency of the scintillation counters was determined by counting one foil of each type in an absolute system. The sulfur foil was counted in a calibrated 2π gas-flow proportional counter, and all of the other foils were counted in a beta-gamma coincidence counting system.

B. PROTON RECOIL NEUTRON SPECTRA MEASUREMENTS

A proton recoil spectrometer was used to determine the differential neutron spectra from ~5 kev to 2.3 Mev at several locations in the shield experiment. These data cover the range between the resonance and threshold region for the foil detectors, and includes a very important portion of the fast reactor shield leakage spectrum. Spherical, gas-filled, proportional counters were used in the manner described by P. W. Benjamin, C. D. Kemshall, and A. Brickstock.⁽⁵⁾ A computer code written by them was used to analyze the raw data taken in the measurements.

The neutron detectors were stainless steel spheres, manufactured by 20th Century Electronics, Ltd.^(6,7) with a 3.94-cm ID and a 0.0508-cm wall thickness. The central anode was a 0.0025-cm tungsten wire. Several detectors were used, each having a different filling of hydrogen, methane, or hydrogen-and-methane gas. Most of the detectors also had a small amount of nitrogen gas for energy calibration. In a thermal neutron flux, the N¹⁴ (n,p) C¹⁴ produces a 615-kev pulse (proton plus carbon-14 ion) which serves as a useful calibration point.

The detectors were operated with a positive high voltage on the anode wire, and with the outer shell grounded. Neutrons entering the detector produce recoil protons in the hydrogeneous fill gas. Each proton ionizes the gas, and the electrons are collected on the central anode wire. The charge collected is proportional to the energy of the proton. Neutrons of a given energy produce recoil protons, continuously distributed in energy from zero to the energy of the neutrons.

In the shielding experiments, there was a large gamma-ray contribution accompanying the neutrons. The gammas strike the detector walls, producing electrons which ionize the gas along with the recoil protons. Since the electrons are less strongly ionizing than protons, they travel much farther for the same energy loss to the gas. The largest energy deposition from an electron corresponds to its traversing the full diameter of the chamber. All energy deposits above this value can only result from recoil protons, while those below can be either neutron- or gamma-induced events. This "cut-off" energy varies with detector gas pressure only, since all the detectors were the same size.

As a result of this cut-off energy, each detector may be used without compensation for gamma-ray background above the cut-off. The influence of gamma rays below this limit depends upon the ratio of neutrons to gamma rays at the point of measurement, and will vary over the shield under test. The lower the gas pressure in a particular chamber, the lower will be the limiting energy. With the lowest pressure detector (0.8 atm H₂), this limit was ~50 kev. Below this energy, gamma-induced events were removed by two-parameter (energy and risetime) gamma discrimination.⁽⁸⁾

Some of the protons strike the wall of the chamber before losing all of their energy, and hence give erroneous pulse height data. The relative number that strike the wall increases as the energy; and hence the range of the protons, increases. Conversely, higher gas pressures decrease the range and increase the useful energy range. Ultimately, these effects establish an upper energy limit for each detector. The computer code of Benjamin *et al.*⁽⁵⁾ calculates an approximate correction for the wall effect, and the limit of this approximation establishes the upper limit for data analysis with each detector. Table 2 gives the detector gas fillings, together with their lower energy limit (for single-parameter analysis) and their upper limit from the wall effect.

TABLE 2
DETECTOR FILLINGS AND ENERGY LIMITS

Fill Gas	Pressure (atm)	E _{min} (Mev)*	E _{max} (Mev)
H ₂	0.8	0.050	0.250
H ₂	2.63	0.100	0.500
CH ₄	0.263		
CH ₄	2.63	0.250	1.2
CH ₄	8.1	0.600	2.3

*E_{min} may be considerably higher than this, in regions where the gamma/neutron ratio is very high.

IV. RESULTS

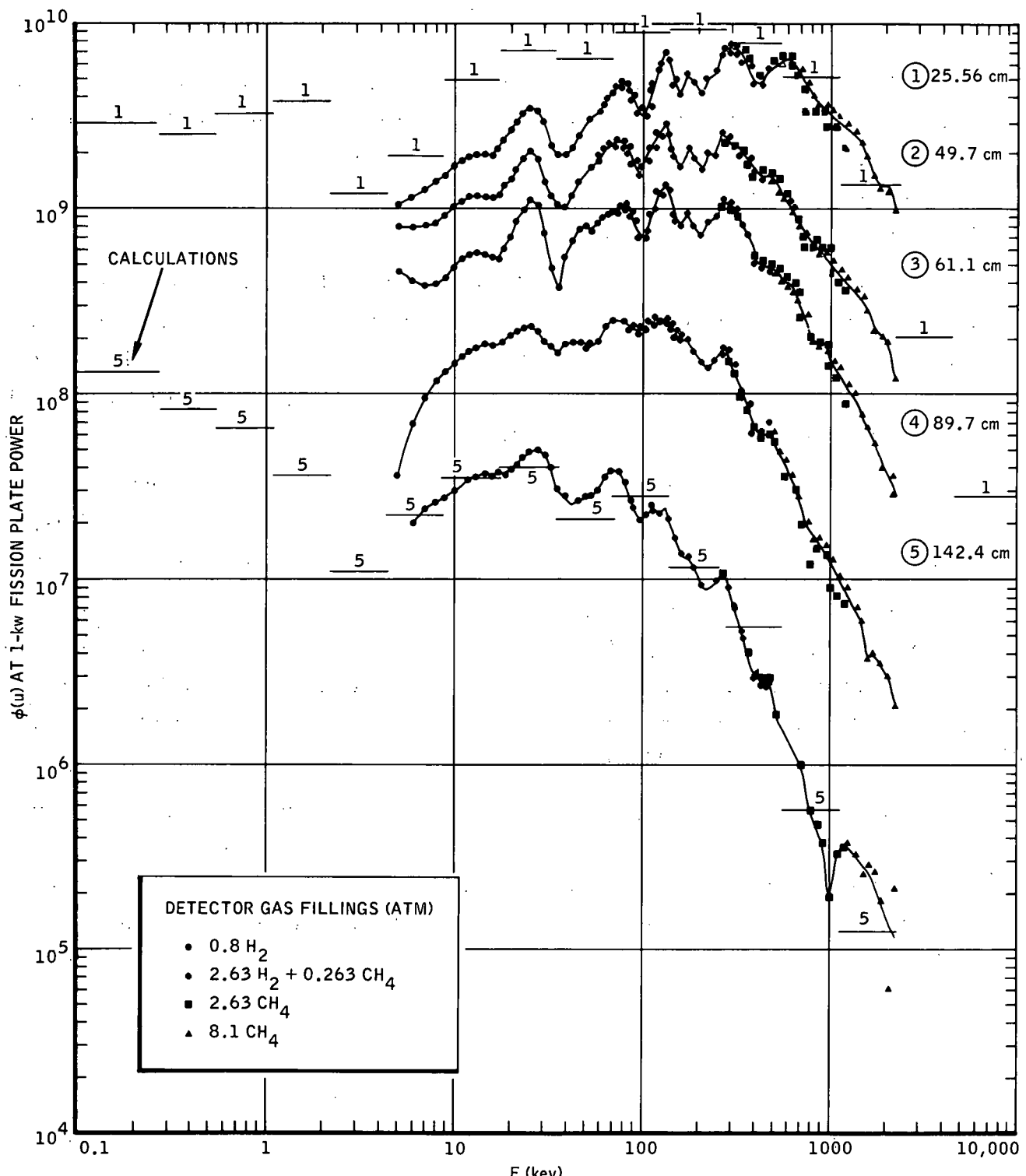
Measurements were made of the neutron spectra and of the activation of indium, gold, cobalt, sulfur, and aluminum foils in a mockup of the region surrounding the FFTF core. Attempts to measure the thermal neutron flux, by using bare and cadmium-covered copper foils, were not successful, because of the very low thermal flux component, in comparison to the resonance flux.

The neutron spectra at five positions in the FFTF radial shield are shown in Figure 5. Data are listed in Tables 3 through 6. The spectra were also measured with a lithium hydride slab replacing the sodium slab following the second stainless steel region. The change in spectra (with the lithium hydride data multiplied by 100) is shown in Figure 6.

The attenuation of neutrons, as measured by use of indium, gold, and cobalt activities, is shown in Figures 7a, b, and c. The fast neutron flux, as measured with sulfur and aluminum detectors, is shown in Figures 8a and b.

The vertical traverses through the shields, using gold and sulfur foils, are shown in Figures 9a through f. The flux shapes indicate positive buckling, with no significant evidence of in-leakage errors. Gold foil data on the lithium hydride interrupt are shown in Figure 7b. The contribution of wall scattered neutrons varies between 4% at 130 cm and 20% at 210 cm.

The statistical errors in the one-parameter proton-recoil data vary uniformly, from about $\pm 1\%$ at the lower energy limit of each detector to about $\pm 10\%$ at the upper energy limit of each detector. Systematic bias in the two-parameter data below 50 kev may be as large as 20% at 26 kev and 50% at 5 kev.



7741-5614

Figure 5. Neutron Spectra in FFTF Radial Shield

AI-AEC-13048

TABLE 3
FFTFS SHIELD SPECTRA
 $\phi(u)$ AT 1-kw F.P. POWER
(0.8 atm H₂ Detector)

E (kev)	25.40 cm		49.54 cm		60.94 cm		89.54 cm		142.24 cm	
	$\phi(u) (10^9)$	% Error	$\phi(u) (10^9)$	% Error	$\phi(u) (10^8)$	% Error	$\phi(u) (10^8)$	% Error	$\phi(u) (10^7)$	% Error
4.96	1.05	0.4	0.795	0.3	4.66	0.3	0.372	0.7	-	-
5.95	1.14	0.5	0.777	0.4	4.05	0.5	0.689	0.6	2.03	0.4
6.94	1.25	0.6	0.796	0.5	3.80	0.7	0.954	0.5	2.41	0.4
7.93	1.37	0.6	0.828	0.6	3.87	0.8	1.14	0.6	2.62	0.5
8.92	1.48	0.7	0.914	0.6	4.20	0.9	1.30	0.6	2.76	0.5
9.91	1.70	0.8	1.02	0.7	4.78	1.0	1.45	0.6	2.98	0.6
10.9	1.81	0.8	1.09	0.7	5.36	1.0	1.58	0.7	3.18	0.6
11.9	1.90	0.9	1.15	0.8	5.59	1.1	1.70	0.7	3.49	0.7
12.9	1.95	1.0	1.17	0.9	5.79	1.2	1.75	0.8	3.62	0.7
14.4	1.96	0.9	1.16	0.8	5.67	1.1	1.86	0.7	3.76	0.6
15.9	1.96	1.5	1.13	1.3	5.48	1.8	1.84	1.1	3.66	1.0
16.9	2.08	1.5	1.15	1.3	5.37	2.1	1.86	1.1	3.73	1.0
18.3	2.34	1.2	1.31	1.1	6.06	1.6	1.93	0.9	3.70	0.9
19.8	2.66	1.6	1.45	1.5	7.11	2.0	2.10	1.3	3.92	1.3
21.3	2.90	1.2	1.61	1.1	8.46	1.5	2.15	1.1	4.08	1.0
23.3	3.20	1.3	1.86	1.1	9.78	1.4	2.24	1.2	4.53	1.0
25.3	3.50	1.3	2.06	1.1	11.30	1.4	2.32	1.3	4.80	1.1
27.8	3.38	1.3	1.86	1.1	10.59	1.4	2.19	1.2	5.08	0.9
30.2	2.90	2.2	1.38	2.2	7.39	2.8	1.91	2.0	4.81	1.3
32.7	2.15	2.6	1.14	2.4	4.81	3.9	1.83	1.9	4.01	1.4
35.7	1.95	3.4	1.04	3.0	3.68	5.9	1.66	2.4	2.98	2.1
38.7	1.94	4.0	0.999	3.7	5.45	4.6	1.88	2.4	2.79	2.5
42.1	2.11	3.5	1.17	3.0	6.63	3.6	1.77	2.4	2.49	2.7
46.1	2.45	3.6	1.41	2.9	7.84	3.6	1.83	2.7	2.64	2.9
50.1	3.22	2.7	1.75	2.0	8.12	4.0	1.85	3.1	2.78	3.1
53.4	3.09	2.7	1.65	2.0	7.71	2.0	1.79	1.8	2.81	1.7
58.4	3.24	3.0	1.79	2.1	8.33	2.1	1.91	2.0	3.02	1.8
63.3	3.72	3.1	2.08	2.1	9.39	2.1	2.30	1.9	3.47	1.8
68.8	4.16	2.7	2.34	1.8	9.74	2.0	2.50	1.7	3.79	1.5
74.9	4.75	2.7	2.40	2.0	9.81	2.3	2.49	1.9	3.84	1.6
81.1	4.85	3.1	2.30	2.4	10.8	2.3	2.46	2.1	3.25	2.1
87.8	4.12	3.6	1.74	3.1	9.37	2.6	2.21	2.3	2.66	2.4
95.8	3.40	4.4	1.72	3.1	7.48	3.3	2.15	2.3	2.06	3.1
104	3.29	5.4	1.93	3.3	6.98	4.1	2.17	2.7	2.26	3.1
113	4.37	4.8	2.22	3.3	9.62	3.5	2.45	2.7	2.45	3.2
123	5.60	3.4	2.61	2.5	12.2	2.5	2.52	2.3	2.36	2.9
134	6.95	3.2	2.85	2.7	13.6	2.5	2.39	2.7	2.44	3.1
146	4.68	5.0	2.03	3.9	9.33	3.7	2.03	3.2	1.80	4.1

TABLE 4
 FFTF SHIELD SPECTRA
 $\phi(u)$ AT 1-kw F.P. POWER
 (2.63 atm H₂ + 0.263 atm CH₄ Detector)

E (kev)	25.40 cm		49.54 cm		60.94 cm		89.54 cm		142.24 cm	
	$\phi(u) \times 10^9$	% Error	$\phi(u) \times 10^9$	% Error	$\phi(u) \times 10^8$	% Error	$\phi(u) \times 10^8$	% Error	$\phi(u) \times 10^7$	% Error
26.5	4.22	0.3	2.18	0.2	11.2	0.2	2.82	0.2	6.17	0.1
29.2	4.18	0.4	2.05	0.3	10.1	0.3	2.68	0.3	5.89	0.2
33.2	3.37	0.4	1.69	0.3	7.61	0.3	2.49	0.3	5.15	0.2
37.1	2.55	0.8	1.39	0.6	6.33	0.6	2.32	0.4	4.32	0.3
39.8	2.68	0.9	1.44	0.7	7.03	0.6	2.33	0.5	4.11	0.4
42.4	2.88	0.9	1.55	0.7	7.99	0.6	2.36	0.5	4.12	0.4
46.4	3.26	0.7	1.69	0.6	8.83	0.5	2.38	0.4	4.18	0.3
50.4	3.43	1.0	1.74	0.8	8.85	0.7	2.27	0.7	3.98	0.5
54.4	3.30	0.9	1.69	0.7	8.36	0.6	2.15	0.6	3.82	0.4
59.7	3.35	1.1	1.89	0.8	8.68	0.7	2.27	0.7	3.96	0.5
65.0	3.78	1.1	2.14	0.8	9.27	0.8	2.63	0.7	4.08	0.5
70.3	4.15	1.2	2.15	0.9	9.41	0.9	2.67	0.7	4.02	0.6
76.9	4.46	1.0	2.20	0.8	9.95	0.7	2.68	0.6	3.68	0.5
83.6	4.56	1.4	2.10	1.2	10.4	1.0	2.52	1.0	3.08	0.8
90.2	3.89	1.5	1.74	1.3	8.70	1.1	2.25	1.0	2.40	0.9
98.1	3.07	2.2	1.53	1.6	7.03	1.5	2.18	1.1	2.12	1.2
106	3.47	2.2	1.78	1.6	7.32	1.7	2.38	1.2	2.17	1.3
115	4.63	1.6	2.14	1.3	9.45	1.2	2.56	1.0	2.28	1.1
126	5.81	1.5	2.47	1.3	12.1	1.1	2.63	1.1	2.22	1.2
137	6.28	1.6	2.49	1.4	12.4	1.2	2.50	1.2	2.09	1.4
149	4.86	1.9	1.90	1.7	8.97	1.5	2.08	1.4	1.64	1.6
162	4.20	2.6	1.73	2.2	8.26	1.9	1.95	1.7	1.34	2.1
176	5.16	2.1	2.08	1.8	9.30	1.7	1.94	1.6	1.29	2.1
192	4.75	2.7	1.88	2.3	8.01	2.2	1.72	2.0	1.16	2.6
208	4.18	3.5	1.64	3.0	7.32	2.8	1.49	2.6	0.908	3.6
225	5.00	3.0	1.95	2.5	8.52	2.3	1.42	2.6	0.881	3.5
245	5.49	2.8	1.97	2.5	8.97	2.2	1.51	2.4	0.975	3.1
267	6.84	2.6	2.54	2.2	10.7	2.1	1.82	2.2	1.10	2.9
289	7.01	2.5	2.43	2.3	10.6	2.1	1.79	2.1	0.975	3.0
314	7.44	2.4	2.22	2.5	9.89	2.1	1.46	2.5	0.683	4.0
342	6.29	3.0	1.97	2.8	8.28	2.5	1.05	3.3	0.501	5.1
373	6.33	3.1	1.88	3.0	7.32	2.9	0.873	3.9	0.387	6.4
406	4.80	4.2	1.57	3.7	5.11	4.1	0.616	5.5	0.347	7.0
440	4.80	4.9	1.44	4.5	4.81	5.0	0.622	6.1	0.276	9.3
479	5.46	4.6	1.49	4.5	4.64	5.3	0.699	5.4	0.266	9.2

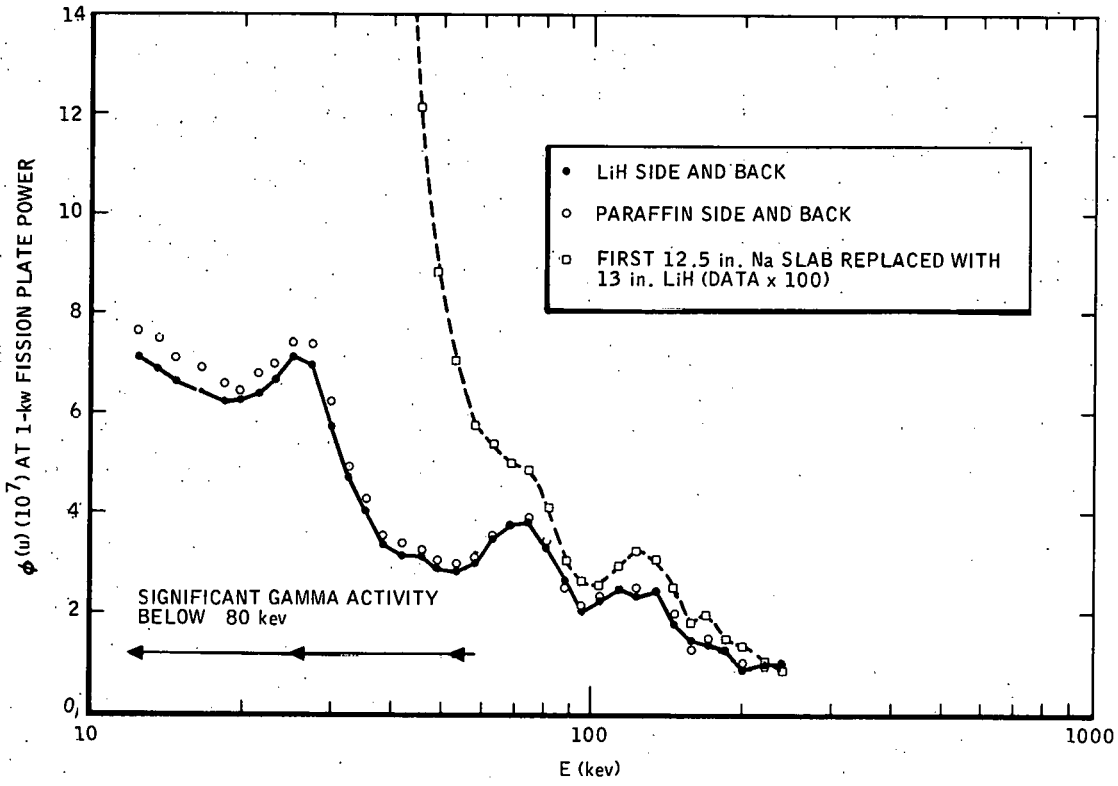
AI-AEC-13048

TABLE 5
 FFTF SHIELD SPECTRA
 $\phi(u)$ AT 1-kw F.P. POWER
 (2.63 atm CH_4 Detector)

E (kev)	25.40 cm		49.54 cm		60.94 cm		89.54 cm		142.24 cm	
	$\phi(u)(10^9)$	% Error	$\phi(u)(10^9)$	% Error	$\phi(u)(10^8)$	% Error	$\phi(u)(10^7)$	% Error	$\phi(u)(10^6)$	% Error
267	7.07	1.0	2.50	0.9	10.4	0.8	16.5	0.9	10.7	1.1
288	7.48	1.1	2.26	1.1	10.1	0.9	15.2	1.0	9.13	1.4
313	7.32	1.0	2.21	1.0	9.47	0.9	12.7	1.0	7.21	1.5
342	7.12	1.2	2.05	1.2	8.29	1.1	9.93	1.4	5.22	2.1
371	6.47	1.5	1.83	1.5	7.28	1.3	7.95	1.9	3.94	2.8
403	4.81	1.9	1.55	1.6	5.53	1.6	6.53	2.0	3.15	3.1
439	5.11	2.1	1.56	1.8	5.08	1.9	5.97	2.4	2.69	3.8
479	5.73	1.8	1.58	1.7	4.85	1.9	5.95	2.2	2.76	3.3
522	5.82	2.0	1.49	1.9	4.79	2.1	5.63	2.5	1.83	5.0
566	6.30	2.1	1.18	2.6	4.23	2.6	3.57	4.0	-	-
612	6.73	1.9	1.09	2.7	3.98	2.6	-	-	-	-
666	5.59	2.2	0.854	3.3	3.54	2.7	2.99	4.1	-	-
724	4.54	2.9	0.706	4.4	2.62	3.9	1.98	6.5	0.987	9.7
789	3.29	3.6	0.607	4.6	2.00	4.4	1.21	9.1	0.561	14.2
857	3.38	4.4	0.658	5.3	1.84	5.9	1.46	9.3	0.473	20.5
929	3.37	4.0	0.608	5.1	1.90	5.0	1.37	8.5	0.368	23.3
1010	2.83	4.9	0.447	7.0	1.46	6.4	0.911	12.4	0.192	46.0
1100	2.75	5.2	0.396	8.2	1.24	7.5	0.808	13.8	0.332	28.0
1200	2.07	8.4	0.379	10.5	0.888	12.3	0.745	17.2	0.349	31.6

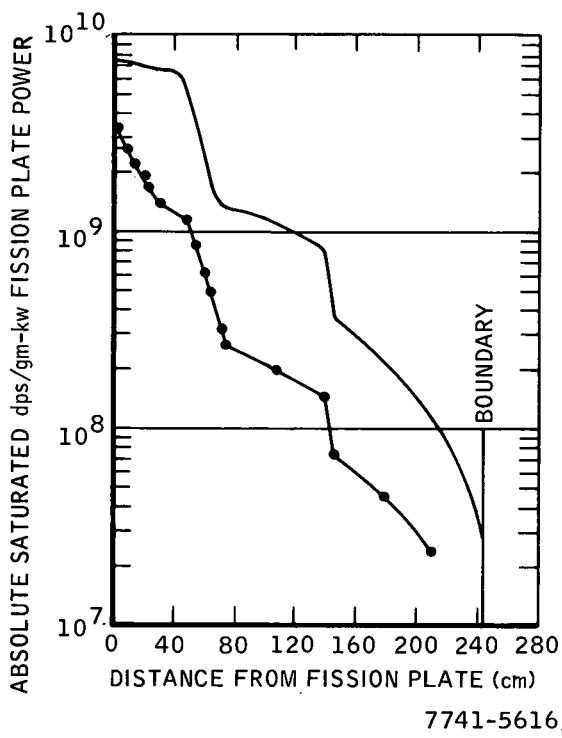
TABLE 6
FFTF SHIELD SPECTRA
 $\phi(u)$ AT 1-kw F.P. POWER
(8.1 atm CH₄ Detector)

E (kev)	25.40 cm		49.54 cm		60.94 cm		89.54 cm		142.24 cm	
	$\phi(u)(10^9)$	% Error	$\phi(u)(10^8)$	% Error	$\phi(u)(10^8)$	% Error	$\phi(u)(10^7)$	% Error	$\phi(u)(10^5)$	% Error
505	5.92	1.0	13.7	0.9	4.58	1.1	6.17	1.1		
547	6.08	1.1	12.2	1.1	4.08	1.3	4.91	1.5		
589	6.38	1.1	11.3	1.3	4.06	1.4	4.38	1.7		
638	6.25	1.0	9.87	1.3	3.71	1.4	3.65	1.8		
694	5.70	1.2	8.42	1.7	3.18	1.7	2.77	2.5		
758	4.90	1.3	7.19	1.9	2.59	1.9	1.99	3.1		
828	4.02	1.8	6.15	2.5	1.96	2.7	1.65	4.1		
898	3.55	2.3	5.70	3.0	1.87	3.1	1.65	4.5		
975	3.58	2.2	5.77	2.8	1.83	3.0	1.51	4.5		
1060	3.28	2.6	5.17	3.4	1.48	4.0	1.33	5.4		
1150	3.17	2.6	4.57	3.7	1.40	3.9	1.03	6.5		
1260	2.81	2.9	4.15	3.9	1.12	4.7	0.891	7.1	3.75	15.2
1370	2.57	3.5	3.63	5.0	0.994	5.7	0.706	9.6	3.23	19.5
1490	2.24	3.9	3.26	5.4	0.769	7.0	0.599	10.8	2.48	25.0
1610	1.89	5.2	2.78	7.0	0.655	9.0	0.374	18.9	2.83	24.3
1750	1.52	5.8	2.14	8.2	0.536	9.8	0.398	16.0	2.59	23.4
1910	1.28	7.9	2.10	9.6	0.387	15.2	0.351	20.1	1.86	35.8
2070	1.29	8.2	1.87	11.0	0.291	20.9	0.301	23.5	0.594	117.1
2250	0.978	12.3	1.20	19.6	0.364	19.0	0.206	38.4	2.12	37.7

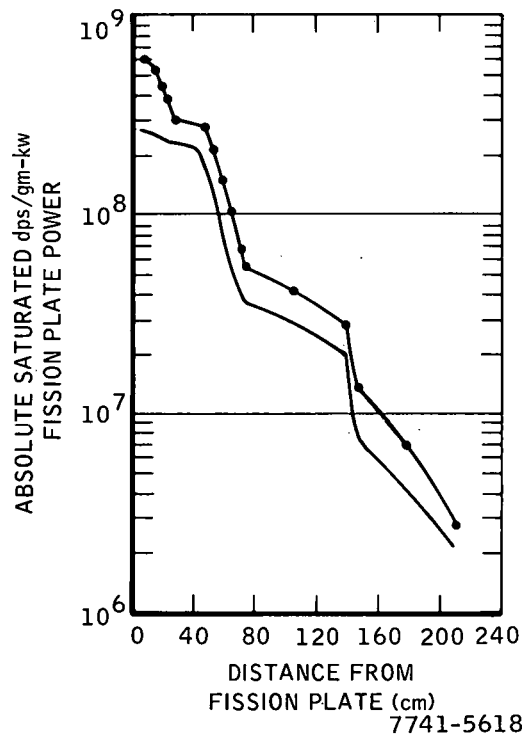


7741-5615

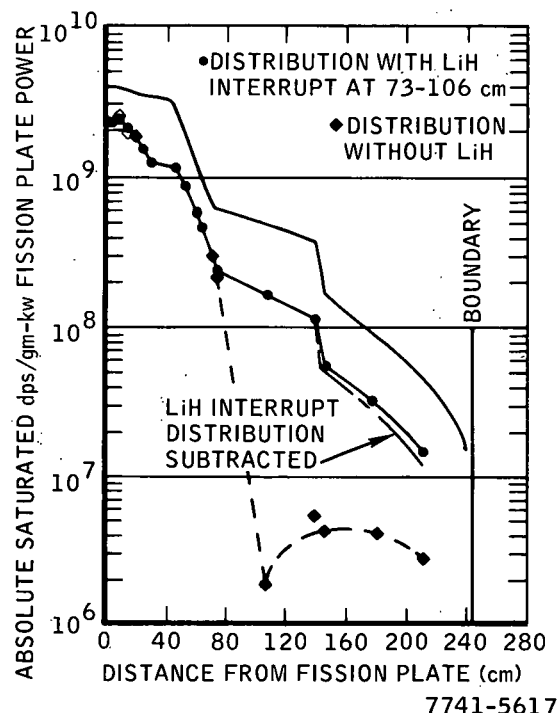
Figure 6. Effect of LiH Interrupt on Neutron Spectrum
in FFTF Radial Shield.



a. Indium Foil

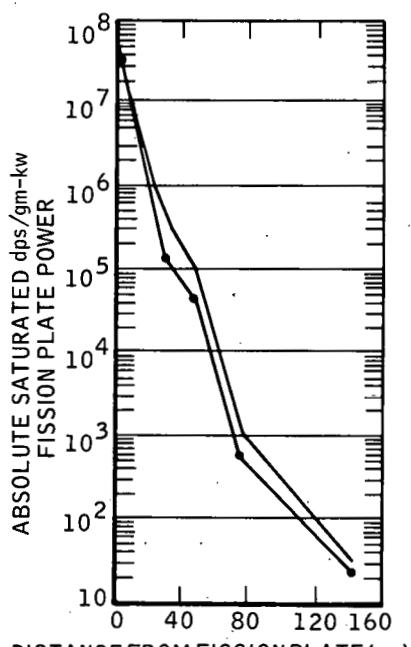


b. Gold Foil



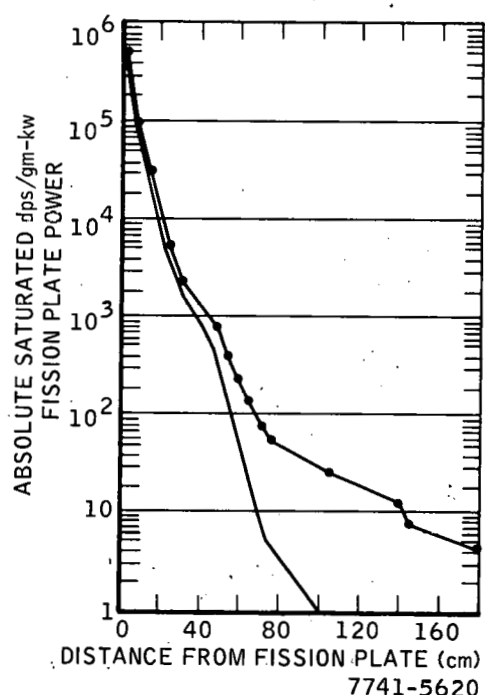
c. Cobalt Foil

Figure 7. Activation in FFTF Radial Shield



a. Sulfur Foil

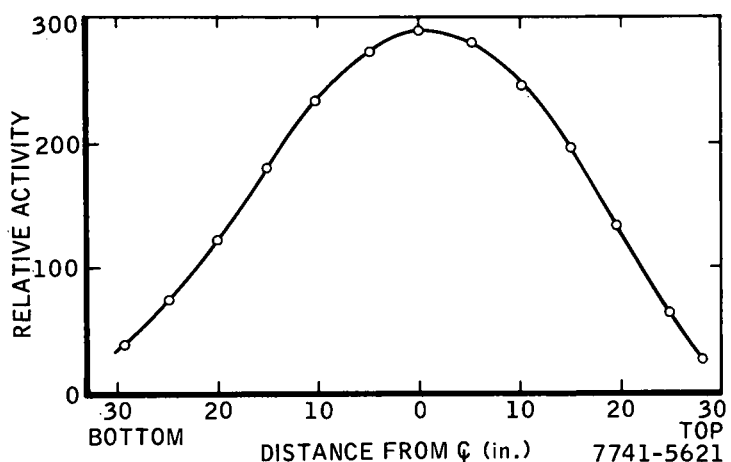
7741-5619



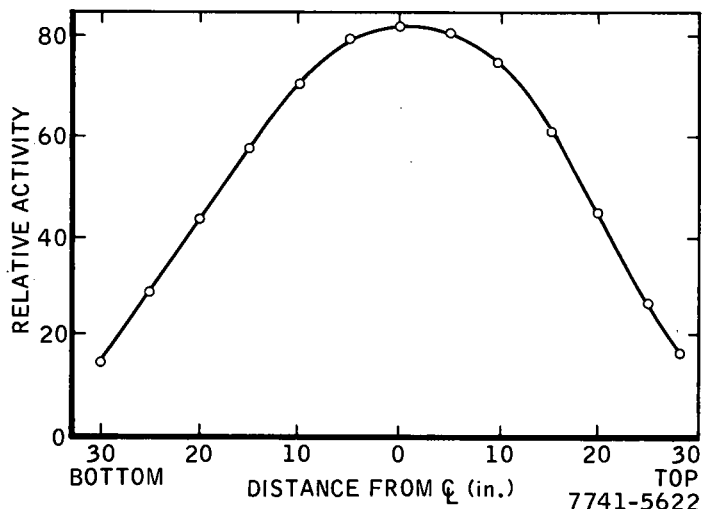
b. Aluminum Foil

7741-5620

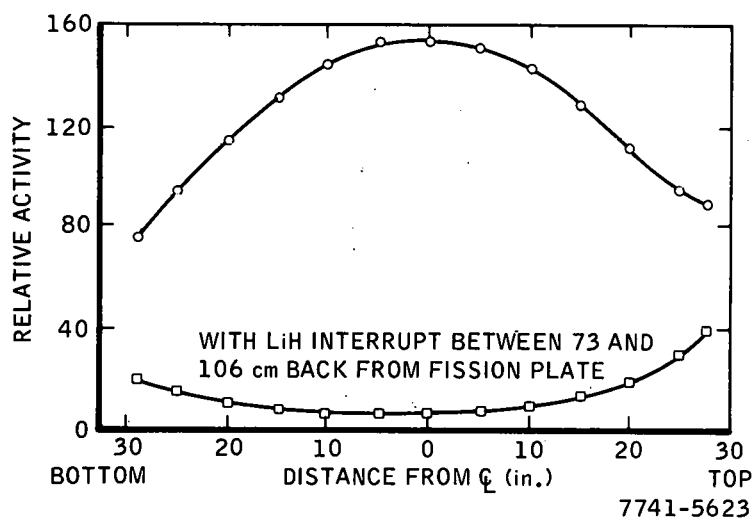
Figure 8. Activation in FFTF Radial Shield



a. Gold Foils, Position 2,
13.7 cm From
Fission Plate

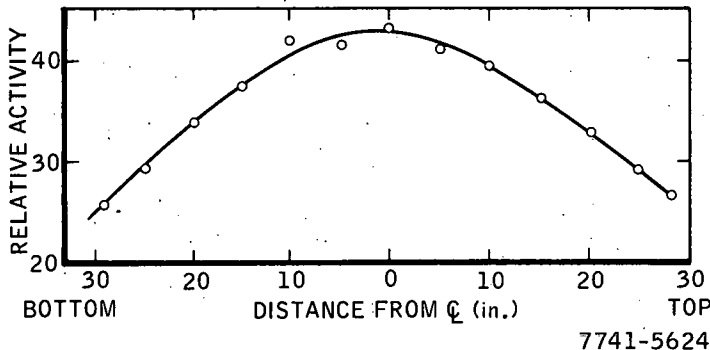


b. Gold Foils, Position 8,
58.1 cm From
Fission Plate



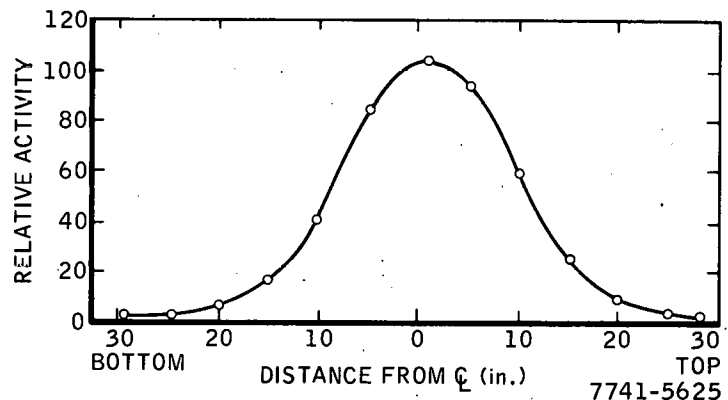
c. Gold Foils, Position 13,
139.1 cm From
Fission Plate

Figure 9. Vertical Traverses in FFTF Radial Shield
(Sheet 1 of 2)



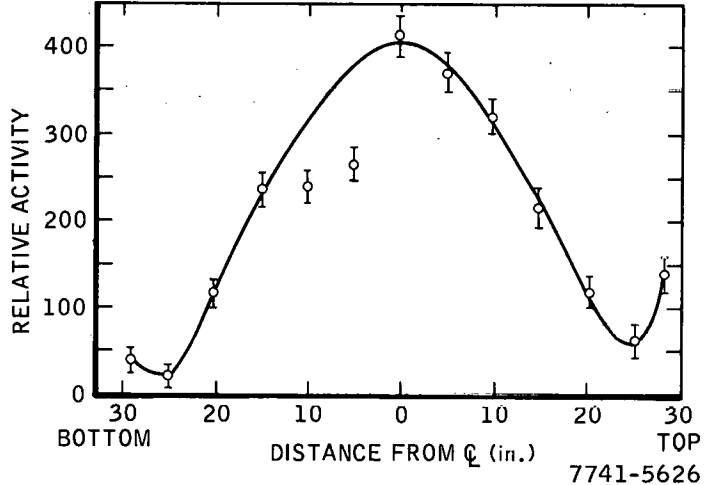
d. Gold Foils, Position 15,
178.1 cm From
Fission Plate

7741-5624



e. Sulfur Foils, Position 5,
28.6 cm From
Fission Plate

7741-5625



f. Sulfur Foils, Position 11,
73.0 cm From
Fission Plate

7741-5626

Figure 9. Vertical Traverses in FFTF Radial Shield

REFERENCES

1. A. W. Thiele, "Neutron and Gamma Ray Attenuation in Sodium Shields," NAA-SR-MEMO-12467 (June 30, 1967)
2. A. W. Thiele, K. G. Golliher, K. L. Rooney, and V. A. Swanson, "Neutron Attenuation Measurements in Sodium-Iron Mixtures Simulating the FFTF Shield," AI-AEC-MEMO-12829 (May 1969)
3. A. W. Thiele, R. J. Cardenas, K. G. Golliher, R. K. Paschall, E. R. Specht, and V. A. Swanson, "Neutron Attenuation Measurements in Shields of Sodium and Steel for Fast Reactor Systems," AI-AEC-MEMO-12838 (June 1969)
4. K. G. Golliher and K. G. Randen, "Capabilities of the 1 Mw Shield Test and Irradiation Reactor," NAA-SR-11528 (1965)
5. P. W. Benjamin, C. D. Kemshall, and A. Brickstock, "The Analysis of Recoil Spectra," AWRE 09/68 (1968)
6. P. W. Benjamin, C. D. Kemshall, and J. Redfearn, "A High Resolution Spherical Proportional Counter," AWRE Report No. NR 1/64 (1964)
7. P. W. Benjamin, C. D. Kemshall, and J. Redfearn, "The Use of a Gas-Filled Spherical Proportional Counter for Neutron Spectrum Measurements in a Zero Energy Fast Reactor," AWRE Report No. NR 2/64 (1964)
8. E. F. Bennett, "Fast Neutron Spectroscopy by Proton Recoil Proportional Counting," Nucl. Sci. Eng 27 (1967) p 16-27



Atomics International
North American Rockwell

P.O. Box 309
Canoga Park, California 91304